Journal of Agricultural Chemistry and Environment, 2026, 15(4), 515-551
https://www.scirp.org/journal/jacen
ISSN Online: 2325-744X
ISSN Print: 2325-7458

Stochastic Modeling of Livestock Herd Dynamics in Agropastoral Households of Burkina Faso: A Monte Carlo Simulation Approach with Log-Normal and Gamma Distributions

Malik Garané[1], Daouda Traoré[2*], Joël Dabiré[3], Drissa Hié[2], Vincent Dah[4]

[1]Training and Research Unit in Legal, Political, Economic and Management Sciences, Department of Economics and Management, Virtual University of Burkina Faso, Ouagadougou, Burkina Faso
[2]Laboratory of Mathematics, Computer Science and Applications (LaMIA), Nazi BONI University, Bobo-Dioulasso, Burkina Faso
[3]Laboratory for Rural Studies on the Environment and Socio-Economic Development, Nazi BONI University, Bobo-Dioulasso, Burkina Faso
[4]Research Laboratory in Economics and Management (LAREM), Nazi BONI University, Bobo-Dioulasso, Burkina Faso
Email: *daoudas704@gmail.com

How to cite this paper: Garané, M., Traoré, D., Dabiré, J., Hié, D. and Dah, V. (2026) Stochastic Modeling of Livestock Herd Dynamics in Agropastoral Households of Burkina Faso: A Monte Carlo Simulation Approach with Log-Normal and Gamma Distributions. *Journal of Agricultural Chemistry and Environment*, **15**, 515-551.
https://doi.org/10.4236/jacen.2026.154028

Received: August 31, 2026
Accepted: November 21, 2026
Published: November 24, 2026

Copyright © 2026 by author(s) and Scientific Research Publishing Inc.
This work is licensed under the Creative Commons Attribution International License (CC BY 4.0).
http://creativecommons.org/licenses/by/4.0/
Open Access

Abstract

Livestock constitutes a critical livelihood asset for agropastoral households in sub-Saharan Africa, yet the stochastic dynamics of herd demography at the household level remain poorly quantified in the Sudanian zone of West Africa. This study develops a stochastic logistic herd dynamics framework applied to six livestock species in 128 agropastoral households of the Province du Tuy, Hauts-Bassins region, Burkina Faso. Four candidate distributions (Log-Normal, Gamma, Weibull, and Inverse Gaussian) were fitted via maximum likelihood estimation and selected by the Akaike Information Criterion, revealing species-specific distributional structures. Demographic rates were estimated from primary survey data and winsorized at biologically grounded ceilings, then propagated through a Monte Carlo simulation ($N = 10000$ replications, $T = 10$ years) to generate the full empirical distribution of final herd sizes, from which Value-at-Risk, Conditional VaR, and extinction probabilities were computed for each species. Non-parametric bootstrap resampling ($B = 5000$) quantified the sampling uncertainty of the parameters of the initial herd-size distributions, and one-at-a-time sensitivity analysis identified birth rates as the dominant driver for poultry and small ruminants, while market transactions govern draft cattle dynamics. Parametric-bootstrap goodness-of-fit tests

did not reject the selected distribution for fattening cattle and sheep only. The risk indicators were insensitive to ±50% changes in the carrying capacities and environmental-noise parameters, but an integer-valued, stock-constrained event model with jointly resampled demographic rates yielded higher quasi-extinction probabilities for all species and did not reproduce the projected growth of sheep and hens. Results reveal a deeply polarized system: fattening cattle follow the only genuinely sustainable trajectory ($r_{\text{net}} = +0.083$; $P(\text{decline}) = 8.5\%$), whereas guinea fowl and draft cattle face critical quasi-extinction risks within a decade ($P(\text{quasi-extinction}) = 47.1\%$ and 28.5% respectively), and apparently growing species such as sheep and hens conceal near-even probabilities of household-level herd contraction that deterministic models would systematically mask, although the magnitude of these risks depends on the specification of the demographic process (see below). These findings provide a probabilistic basis for designing species-differentiated livestock interventions in agropastoral systems of the Sahel.

Keywords

Stochastic Modeling, Monte Carlo Simulation, Livestock Herd Dynamics, Log-Normal Distribution, Gamma Distribution, Value-at-Risk, Agropastoral Households, Burkina Faso

1. Introduction

Livestock farming is a cornerstone of rural livelihoods in West Africa, providing food, income and savings to agropastoral households. In Burkina Faso, cattle and poultry production systems are central to rural livelihoods and to agricultural value added [1]. Yet herd dynamics in smallholder systems are inherently stochastic, driven by climatic shocks, market volatility, disease outbreaks, and structural constraints such as limited veterinary access and degraded pastures [2] [3].

Deterministic models of herd growth do not capture the high variability observed in household-level data; in the present survey, the coefficients of variation of herd sizes range from 50% to 104% (Section 4.1). Probabilistic and simulation-based approaches offer a more realistic representation of this uncertainty. Climate-related risks to livestock systems in developing countries are well documented [4], but a review of 126 farm household models showed that such models remain weak on risk analysis [5], and household-level stochastic risk assessment remains rare in West Africa. Recent work on stochastic population models has also highlighted the role of distributional choices for population sizes and counts [6] [7].

Despite these methodological advances, a species-specific, household-level stochastic logistic approach that integrates formal risk indicators such as Value-at-Risk (VaR) and Conditional Value-at-Risk (CVaR) is still lacking in the context of agropastoral systems in Burkina Faso.

Furthermore, our study aims to achieve the following objectives:

1) To fit four candidate distributions (Log-Normal, Gamma, Weibull, Inverse Gaussian) via maximum likelihood estimation (MLE) with AIC-based selection, using primary survey data from 128 agropastoral households.

2) To simulate 10-year herd trajectories for six livestock species (draft cattle, fattening cattle, sheep, goats, hens, guinea fowl) using a stochastic logistic growth model with winsorized demographic rates.

3) To compute species-specific risk indicators, including Value-at-Risk (VaR), Conditional VaR (CVaR), probability of decline, and quasi-extinction probability.

4) To perform a one-at-a-time (OAT) sensitivity analysis to rank the influence of birth, death, sale, purchase, and consumption rates on final herd size.

5) To assess the robustness of the risk indicators to the integer-valued nature of herd sizes, to the independence assumption on demographic rates, and to the carrying-capacity and environmental-noise assumptions.

The structure of this article is organized as follows. Section 2 reviews the existing literature on stochastic livestock modeling, distribution fitting, and risk assessment in dryland systems. Section 3 describes the study area, survey data, demographic rate estimation, the stochastic logistic model, Monte Carlo simulation design, bootstrap inference, and the OAT sensitivity analysis. Section 4 presents the descriptive statistics, distribution fitting outcomes, winsorized demographic rates, simulation trajectories, risk indicators, bootstrap confidence intervals, and sensitivity analysis results. Section 5 interprets the findings, derives policy implications, and acknowledges limitations. Finally, Section 6 concludes and suggests avenues for future research.

2. Literature Review

The stochastic nature of livestock herd dynamics in smallholder systems has received increasing attention. Lesnoff *et al*. (2012) [2] used a herd growth model and a global sensitivity analysis to simulate the post-drought recovery of a Sahelian cattle population, and showed that the recovery time is extremely variable and depends mainly on the magnitude of the drought-induced decline, the calving rate and farmers' offtake strategy. In Burkina Faso, Sanou *et al*. (2025) [3] combined climate records (1961-2020) and veterinary data (2003-2019) to show that climate patterns influence the occurrence of major livestock diseases across the Sahelian, Sudano-Sahelian and Sudanian zones, a source of shocks that deterministic projections ignore.

A key methodological challenge in stochastic herd modeling is the selection of an appropriate probability distribution for herd sizes, demographic rates, or environmental noise. The Log-Normal distribution naturally accommodates positive, right-skewed data [8]. The Gamma distribution has been used to summarise caprine age-at-death profiles, for which it provided a simpler and better-fitting model than idealised kill-off profiles [9]. For discrete-time stochastic logistic populations, Wang (2024) [6] showed that the stationary distribution of population

size can be described by a Gamma distribution whose parameters are explicitly related to the intrinsic growth rate and to the variance of the perturbations. For count data with excess zeros, Batardière *et al*. (2025) [7] extended the multivariate Poisson-lognormal model to zero inflation, and Sartore *et al*. (2020) [10] modelled monthly swine inventories by combining survey estimates with the biological dynamics of the herd. These studies illustrate that the appropriate distribution depends on the population and data considered, which is consistent with the species-specific selection adopted here.

Stochastic and nonlinear population models have also been applied to livestock and related populations. Arlot *et al*. (2019) [11] coupled the Yoccoz-Birkeland population model with price dynamics and showed that it generates chaotic cycles in livestock commodity markets. Hamnett *et al*. (2024) [12] used a stochastic Leslie matrix with density feedback to identify cost-effective harvest strategies for feral pig eradication over 3- and 10-year horizons. These works underscore the importance of combining density dependence and stochasticity, as attempted in the present study.

In West Africa, several modeling efforts have focused on crop-livestock integration and farm trajectories. Assogba *et al*. (2026) [13] developed TENGA, an agent-based model simulating 700 heterogeneous farms in semi-arid Burkina Faso, and used a Morris sensitivity analysis to explore crop-livestock integration scenarios. Cosme *et al*. (2024) [14] used the qualitative EDEN discrete-event framework to identify the conditions under which a poorly endowed farm of southwestern Burkina Faso can develop sustainable agropastoralism. Neither study reports downside risk indicators such as VaR or CVaR. In Namibia, Dressler *et al*. (2025) [15] developed an agent-based model of a communal pastoral rangeland to analyse the effects of population density and of climate and income shocks on livelihoods and rangeland condition. Agent-based models are, however, data-intensive and difficult to calibrate for household surveys with moderate sample sizes, which motivates our simpler, directly parametric Monte Carlo approach.

Risk assessment in livestock systems has traditionally relied on variance-based measures, whereas downside risk metrics focus on the lower tail of the outcome distribution. Climate change is expected to affect livestock systems in developing countries through feed, water, heat stress and disease [4], and structural Ricardian analyses of African livestock farms indicate that warming reduces livestock net income and induces adaptation in species choice [16]. Value-at-Risk and Conditional VaR, developed in finance, summarise the lower tail of an outcome distribution, while in population viability analysis the probability of falling below a critical threshold (quasi-extinction) is a standard risk indicator [17]. Both types of indicators are reported in this paper.

Sensitivity analysis is an essential step in stochastic modeling to identify which inputs drive the uncertainty of the outputs. Puech (2024) [18] developed a viability algorithm to assess the robustness and adaptability of mixed ruminant herds (dairy cattle and suckler sheep) under combined meteorological and economic

hazards. Springbett *et al*. (2003) [19] used stochastic simulations of a compartmental epidemic model to show that genetic heterogeneity in livestock populations reduces the probability of catastrophic epidemics. Srivastava *et al*. (2025) [20] integrated crop, grassland and livestock models across West Africa and projected declines in livestock numbers of up to 43% in the northern Sahelian zone under climate change. OAT analysis, as implemented in our study, is computationally efficient and provides a clear ranking of parameter importance, though it may miss interaction effects that would require more advanced methods such as Sobol indices.

Despite the growing body of stochastic livestock models, a framework that simultaneously combines i) distribution fitting with AIC selection, ii) a discrete-time stochastic logistic process, iii) formal downside risk indicators (VaR, CVaR), iv) bootstrap confidence intervals, and v) OAT sensitivity analysis has not yet been applied to agropastoral households in Burkina Faso. Bayesian methods for comparing Log-Normal populations, such as intrinsic priors for testing two lognormal means [21] and credible intervals for the lognormal median [22], have not been applied to herd-size distributions from West African survey data, and the Gamma modelling of caprine age-at-death profiles [9] did not address future herd trajectories.

Therefore, to the best of our knowledge, no previous study has simultaneously combined all these methodological elements into a single Monte Carlo simulation framework with empirically calibrated distributions and formal tail risk metrics for the six main livestock species in Burkinabè agropastoral systems. Our article explicitly addresses this gap by proposing a stochastic logistic model parameterized with primary survey data from 128 households, covering draft cattle, fattening cattle, sheep, goats, hens, and guinea fowl.

3. Methodology

3.1. Study Area

The study was conducted in the localities of Gombèlèdougou and Koumbia, Province of Tuy, Hauts-Bassins region, southwestern Burkina Faso (**Figure 1**). This area lies within the Sudanian climatic zone (South-Sudanian for Gombèlèdougou, transitional for Koumbia), characterized by a rainy season from May/June to October (peak rainfall in July-August) and a dry season from November to April, including the harmattan period (November-February) and a hot, arid phase (March-May). Mean annual rainfall ranges from 800 to 1100 mm, and mean annual temperatures exceed 2528, with maxima reaching 4045 between March and May. This climate supports both cash and cereal crops, making the area one of the most productive agricultural zones in Burkina Faso.

Agropastoral activity in the study area is characterized by mixed farming, where crop production coexists with cattle, small ruminants, and poultry. Land and natural resource competition between farmers and herders is intense, driven by population growth, rangeland degradation, and the expansion of cultivated fields into

traditional grazing areas and pastoral corridors. These structural pressures, combined with climatic variability, create a highly uncertain environment for livestock management, justifying the stochastic modeling approach of this study. Primary data were collected through a structured household survey of $n = 128$ agropastoral households across the two localities, covering herd composition by species, annual demographic flows (births, deaths, sales, purchases, own consumption), feeding and watering practices, veterinary care, and labor allocation.

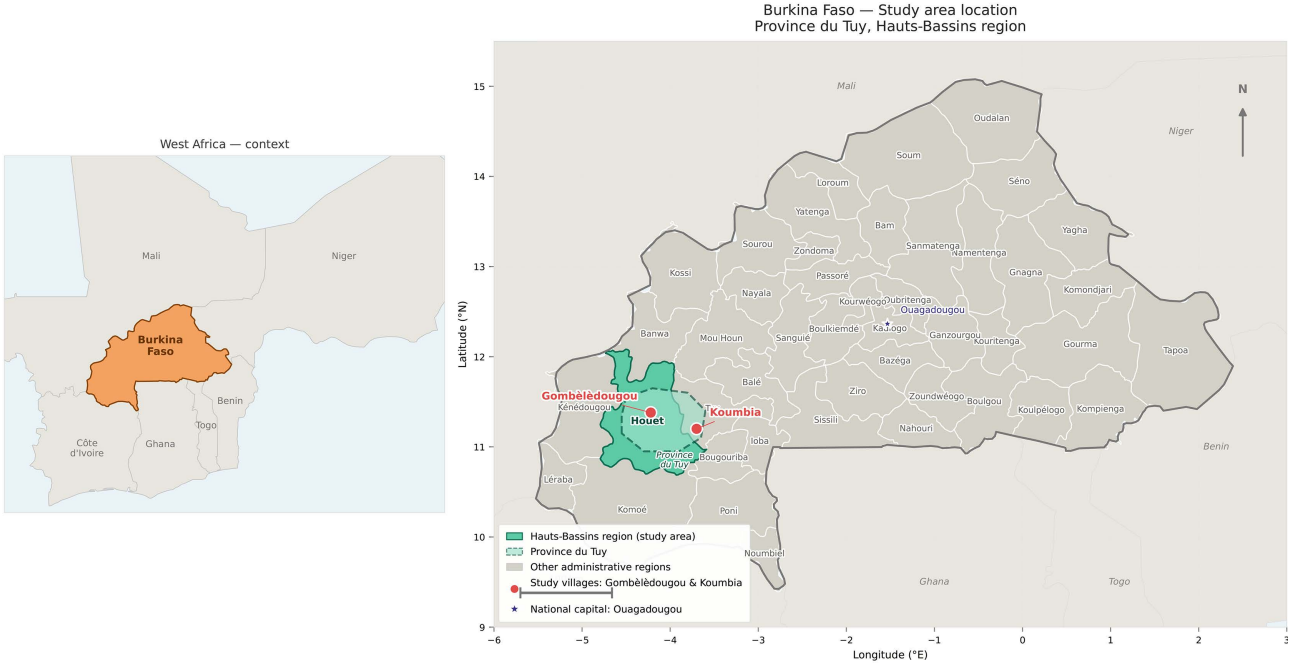

Figure 1. Location of the study area in Burkina Faso. *Left panel*: position of Burkina Faso within West Africa. *Right panel*: the 13 administrative regions of Burkina Faso; the Hauts-Bassins region (shaded green) contains the Province du Tuy (dashed boundary), where the two study localities Gombèlèdougou and Koumbia are situated. Primary data were collected from $n = 128$ agropastoral households across both localities. Source: Natural Earth 1:10m; coordinates in WGS84.

3.2. Survey Design, Sampling Frame and Data Quality

The target population consisted of the heads of family farms practising livestock keeping in Gombèlèdougou and Koumbia, which count approximately 400 and 800 family farms, respectively [23]. The sampling frame was the list of farms established with the local veterinary services, the livestock-keeper groups and the village chiefs. Households were selected purposively, not at random, among the members of the cotton producer groups and livestock-keeper groups, the main producer organizations of the two villages, on the basis of a preliminary qualitative phase and of a farm typology based on cultivated area and cattle numbers (farmers: fewer than 10 cattle; agro-pastoralists: more than 10 cattle and more than 5 ha cultivated; pastoralists: more than 10 cattle and less than 5 ha cultivated). To cover the diversity of farms, members of the cotton producer groups cultivating less than 5 ha, 5 to 15 ha and more than 15 ha, and members of the livestock-keeper groups owning 10 to 20 and more than 20 cattle, were included. This procedure

yielded $n = 128$ households, about 10% of the family farms of each village (44 in Gombèlèdougou and 84 in Koumbia). Data were collected with a structured questionnaire covering the general and structural characteristics of the farm, livestock practices and production constraints. The survey was conducted during the post-harvest period by enumerators trained beforehand on the questionnaire, the definitions of the variables and interviewing techniques; each questionnaire was completed during an individual interview lasting 60 to 90 minutes, and the data were checked daily in the field to detect and correct errors or inconsistencies.

Annual demographic flows (births, deaths, sales, purchases and own consumption) were collected retrospectively for each livestock category; conducting the survey after harvest allowed respondents to report on the complete preceding year. Herd sizes are those reported at the interview, and this stock defines X in the rate computations of Section 3.5.

In the raw data, herd size was missing for 2 households for fattening cattle, 1 for sheep, 10 for hens and 9 for guinea fowl, and none for draft cattle and goats. Among herd-owning households, demographic flows were missing for 9 to 11 households for draft cattle, 2 to 4 for fattening cattle, 4 for sheep, 5 to 7 for goats, 2 to 6 for hens and 1 to 2 for guinea fowl, depending on the flow. Missing herd sizes and flows were imputed by the sample mean of the corresponding variable, except for sheep and goat herd sizes, which were not imputed (the single missing sheep herd size was excluded). As a consequence, households with an unknown herd size were treated as owners, and the herd-size samples analysed in Section 4.1 include 2 mean-imputed values for fattening cattle, 10 for hens and 9 for guinea fowl; this explains the non-integer medians of fattening cattle and hens. The integer-valued analyses (Section 4.2 and Section 3.7) use only the observed, non-imputed herd sizes. Households not owning a given category were excluded from the analyses of that category, which explains the species-specific sample sizes reported in Section 4.1. The three missing values on education level (Section 4.1) concern a socio-demographic covariate only and do not enter the demographic model.

3.3. Definition of the Livestock Categories

The six categories analyzed are functional production categories as declared by the respondents, not sex- and age-specific animal groups. Draft cattle are animals kept primarily for animal traction (ploughing and transport); fattening cattle designate the other cattle of the household herd, kept for production and sale. Sheep, goats, hens and guinea fowl refer to the whole flock of each species. The questionnaire recorded the number of animals by sex and age class (<1, 1 - 5, 6 - 10 and >10) for cattle and small ruminants, but not for poultry. The resulting composition (**Table 1**) shows that draft cattle consist almost exclusively of males of age class ≥1 (96.9%), whereas the fattening cattle category is dominated by females of age class ≥1 (67.0%) and includes young animals (15.2%); it therefore contains the breeding females of the household cattle herd, which explains its non-zero birth rate.

Births were recorded at the category level. The birth rate used in the model is therefore a crude rate per head of the category, $r_{\text{birth}} = F_{\text{birth}} / X$, which equals the per-female birth rate multiplied by the proportion of breeding females in the category. Applying this crude rate in the projections assumes that the sex-age composition of each category remains approximately stationary over the simulation horizon. Expressed per female of age class ≥1, the birth rate is 0.44 for draft cattle, 0.22 for fattening cattle, 0.55 for sheep and 0.49 for goats (Table 1). For draft cattle, the very low crude birth rate (0.011) thus results from the near-absence of females in the category (2.4% of animals, 10 females in total) rather than from low fecundity; the dynamics of this category are accordingly driven by purchases, sales and replacement rather than by reproduction.

Table 1. Sex-age composition of the livestock categories (herd-owning households; percentage of animals) and birth rate per female of age class ≥1.

Category	Males ≥ 1 (%)	Females ≥ 1 (%)	Young < 1 (%)	Births per female ≥ 1
Draft Cattle	96.9	2.4	0.7	0.44
Fattening Cattle	17.8	67.0	15.2	0.22
Sheep	13.4	58.5	28.1	0.55
Goats	18.8	60.1	21.2	0.49
Hens	–	–	–	–
Guinea Fowl	–	–	–	–

Age classes as coded in the questionnaire (<1, 1 - 5, 6 - 10, >10); ≥1 groups the three upper classes. Goats: the class of males <1 is absent from the data file, so that the young of goats are females only. Hens and guinea fowl: sex and age not recorded. Births per female = total births of the category/total females of age class ≥1.

3.4. Distribution Fitting

Let X denote the herd size of a randomly selected household for a given species. Given the positive, right-skewed nature of livestock counts, four parametric distributions were fitted via maximum likelihood estimation (MLE). The Log-Normal distribution (Equation 1) is commonly used for positively skewed biological data because it results from the product of many independent positive factors [8]. The Gamma distribution (Equation 2) offers flexibility for moderate skewness and has been applied to age-at-death profiles in livestock [9]. The Weibull distribution (Equation 3) is often used in survival and reliability analysis [24]. The Inverse Gaussian distribution (Equation 4) is suitable for highly concentrated, heavy-tailed herd sizes [25].

$$f\left(x;\mu,\sigma\right) = \frac{1}{x\sigma\sqrt{2\pi}} \exp\left(-\frac{\left(\ln x - \mu\right)^2}{2\sigma^2}\right), \quad x > 0 \tag{1}$$

$$f(x;\alpha,\beta)=\frac{x^{\alpha-1}\mathrm{e}^{-x/\beta}}{\beta^{\alpha}\Gamma(\alpha)},\ x>0 \tag{2}$$

$$f(x;c,\lambda)=\frac{c}{\lambda}\left(\frac{x}{\lambda}\right)^{c-1}\exp\left(-\left(\frac{x}{\lambda}\right)^{c}\right),\ x>0 \tag{3}$$

$$f(x;\mu,\lambda)=\sqrt{\frac{\lambda}{2\pi x^{3}}}\exp\left(-\frac{\lambda(x-\mu)^{2}}{2\mu^{2}x}\right),\ x>0 \tag{4}$$

Model selection was based on the Akaike Information Criterion ($\mathrm{AIC}=-2\hat{\ell}+2k$) and the Bayesian Information Criterion ($\mathrm{BIC}=-2\hat{\ell}+k\ln n$), where $\hat{\ell}$ is the maximized log-likelihood and $k=2$ (number of parameters). Goodness-of-fit was first assessed with the Kolmogorov-Smirnov (KS) test. Because the parameters are estimated from the same data, the nominal KS p-values are not valid (they are conservative) [26]. We therefore computed parametric-bootstrap p-values [27]: for each species and candidate distribution, $B_{\mathrm{GOF}}=1000$ samples of size n were drawn from the fitted distribution, the distribution was re-estimated by MLE on each sample, and the KS statistic D_b^{*} was recomputed; the p-value is $\left(1+\#\left\{b: D_b^{*}\geq D_{\mathrm{obs}}\right\}\right)/\left(B_{\mathrm{GOF}}+1\right)$. Since herd sizes are counts, ties make the continuous KS test only approximate, which motivates the integer-valued sensitivity analysis described below.

Parameterization. All parameters are reported in the parameterization of Equations (1)-(4). Estimation was performed with scipy.stats with the location parameter fixed at zero, and the software parameters were converted as follows: lognorm (s,scale): $\sigma=s$, $\mu=\ln(\mathrm{scale})$; gamma (a,scale): $\alpha=a$, $\beta=\mathrm{scale}$; weibull_min (c,scale): $c=c$, $\lambda=\mathrm{scale}$; invgauss (m,scale): $\mu=m\cdot\mathrm{scale}$, $\lambda=\mathrm{scale}$.

Integer-valued sensitivity analysis. Because herd sizes among owners are integers $x\geq 1$, two zero-truncated count distributions were also fitted by MLE [28]: the zero-truncated Poisson (ZTP) and the zero-truncated negative binomial (ZTNB),

$$P(X=x)=\frac{g(x)}{1-g(0)},\ x=1,2,\cdots, \tag{5}$$

where g is the Poisson (θ) probability mass function or the negative binomial mass function $g(x;m,k)=\frac{\Gamma(x+k)}{\Gamma(k)x!}\left(\frac{k}{k+m}\right)^{k}\left(\frac{m}{k+m}\right)^{x}$, with mean m and dispersion k ($\mathrm{Var}=m+m^{2}/k$). Zero inflation is not relevant here because only herd-owning households are modeled. These distributions were fitted to the observed (non-imputed) integer herd sizes. AIC values of discrete and continuous models are not comparable (probability mass versus density), so the two discrete candidates were compared with each other, their fit was assessed with a parametric-bootstrap KS test on the discrete distribution function, and the retained discrete distribution was used to draw integer initial herd sizes in the event model of Section 3.7.

3.5. Winsorized Demographic Rate Estimation

To obtain robust estimates of demographic rates (births, deaths, sales, purchases, own consumption) for each species, we first computed annual rates as $r_j = F_j / X$ for herd-owning households, where F_j is the observed annual flow of type j and X the initial herd size. However, raw rates can be unrealistically high for households with very small herds. To mitigate this, we applied winsorization at species-specific biological ceilings c_j derived from West African livestock literature [2]:

$$r_j^w = \min\left(r_j, c_j\right) \tag{6}$$

The winsorized mean $\bar{r}_j^w$ and standard deviation s_j^w were then calculated (Section 4.3) and used as parameters of a Normal distribution for each rate in the simulation. This approach prevents extreme demographic events from dominating the simulated trajectories while preserving the observed variability.

3.6. Stochastic Logistic Growth Model

Herd dynamics were modeled as a discrete-time stochastic logistic process, a framework widely applied to animal populations under environmental uncertainty [6]. The model is written as:

$$X_{t+1} = X_t \cdot \exp\left[r_{\text{net},t}\left(1 - \frac{X_t}{K}\right) + \varepsilon_t \right] \tag{7}$$

where:

- $r_{\text{net},t} = r_{\text{birth},t} + r_{\text{purch},t} - r_{\text{sale},t} - r_{\text{death},t} - r_{\text{cons},t}$, clipped to the interval $[-1.5, 1.5]$ to avoid biologically implausible growth or collapse;
- each demographic rate $r_{j,t}$ is drawn independently at each time step from a Normal distribution: $r_{j,t} \sim \mathcal{N}\left(\bar{r}_j^w, \left(s_j^w\right)^2\right)$, then clipped to $\left[0, c_j\right]$, independently of the other rates. This independence is an approximation: sales, deaths, own consumption, births and purchases may be correlated (e.g. distress sales following mortality shocks) and are jointly constrained by the available stock. Its consequences are assessed with the stock-constrained event model of Section 3.7;
- K is the species-specific carrying capacity, interpreted as the maximum herd size a household can maintain given its land, labor, feed and housing resources. The values used (**Table 2**) were fixed by the authors as upper bounds exceeding the largest herd size observed for each species (Section 4.1); they were neither estimated from the survey data nor obtained through a formal elicitation procedure. Because K is not directly observed, the sensitivity of the conclusions to alternative capacities is assessed (Section 3.9);
- $\varepsilon_t \sim \mathcal{N}\left(0, \sigma_{\text{env},s}^2\right)$ represents environmental stochasticity (e.g., drought, disease outbreaks). The species-specific values $\sigma_{\text{env},s}$, ranging from 0.04 for draft cattle to 0.08 for poultry (**Table 2**), were fixed by assumption, with larger values for short-cycle species; they were not calibrated on rainfall or mortality series. Their influence on the results is assessed in Section 3.9.

Initial herd sizes X_0 were drawn from the best-fit distribution for each species (Section 4.2) and truncated to the interval $[1, K]$; in addition, simulated herd

sizes were bounded above by $2K$ at each time step.

Table 2. Carrying capacities K and environmental-noise parameters $\sigma_{\text{env},s}$ used in the simulations.

Species	K	Maximum observed herd size	$\sigma_{\text{env},s}$
Draft Cattle	15	10	0.04
Fattening Cattle	120	96	0.05
Sheep	80	46	0.06
Goats	80	40	0.06
Hens	150	80	0.08
Guinea Fowl	60	20	0.08

K and $\sigma_{\text{env},s}$ were fixed by the authors (not estimated); their influence is assessed in Section 4.8.

Monte Carlo simulation was performed with $N = 10000$ independent replications over a 10-year horizon (i.e., 10 annual time steps), which is sufficient to obtain stable risk estimates [29].

3.7. Integer-Valued Stock-Constrained Event Model

To assess jointly i) the continuous approximation of herd size and ii) the independent sampling of demographic rates, we implemented an alternative event-based model used as a robustness check. Initial herd sizes $X_0 \in \{1, 2, \cdots\}$ are drawn from the retained zero-truncated count distribution (Equation 5). In each year t and each trajectory, a complete vector of rates $\boldsymbol{r}_t = \left(r_{\text{birth}}, r_{\text{death}}, r_{\text{sale}}, r_{\text{purch}}, r_{\text{cons}}\right)_t$ is obtained by resampling the observed winsorized rate vector of one surveyed household, which preserves the empirical cross-correlations among flows. Events are then generated sequentially and constrained by the available stock:

$$\begin{aligned} D_t &\sim \text{Bin}\left(X_t, \min\left\{1, r_{\text{death},t} \mathrm{e}^{-\varepsilon_t}\right\}\right), \\ \left(S_t, C_t\right) &\sim \text{Mult}\left(X_t - D_t; \pi_{\text{sale},t}, \pi_{\text{cons},t}\right), \\ B_t &\sim \text{Poisson}\left(r_{\text{birth},t} \mathrm{e}^{\varepsilon_t} X_t \left(1 - X_t / K\right)_+\right), \\ P_t &\sim \text{Poisson}\left(r_{\text{purch},t} X_t \left(1 - X_t / K\right)_+\right), \\ X_{t+1} &= X_t - D_t - S_t - C_t + B_t + P_t, \end{aligned} \tag{8}$$

where $\varepsilon_t \sim \mathcal{N}\left(0, \sigma^2_{\text{env},s}\right)$, $\left(\pi_{\text{sale},t}, \pi_{\text{cons},t}\right) = \left(r_{\text{sale},t}, r_{\text{cons},t}\right)$ rescaled to sum to at most one, and $(u)_+ = \max(u, 0)$. By construction, deaths, sales and own consumption can never exceed the stock present, and X_t remains a non-negative integer. The same horizon ($T = 10$), number of replications ($N = 10000$) and risk indicators as in the baseline model are used, and the two specifications are compared in Section 4.8.

3.8. Risk Indicators

To quantify downside risk, we computed two complementary metrics. Let $R = (X_T - X_0)/X_0$ denote the household-level relative change in herd size over the horizon. Throughout the paper, Value-at-Risk (VaR) is defined as a lower-tail *return* quantile, not as a positive loss: for a confidence level q (here $q = 0.95$),

$$\mathrm{VaR}_q = Q_{1-q}(R), \tag{9}$$

So that VaR_{95} is the 5th percentile of R. Negative values indicate losses: $\mathrm{VaR}_{95} = -x\%$ means that 5% of the simulated household trajectories lose more than $x\%$ of their initial herd. Conditional VaR (CVaR), also known as Expected Shortfall, is the mean relative change within this lower tail:

$$\mathrm{CVaR}_q = \mathbb{E}\left[R \mid R \le \mathrm{VaR}_q\right]. \tag{10}$$

Both measures are thus expressed on the same signed scale as R; a more negative value indicates a higher downside risk. Two growth summaries are also distinguished because they differ in general: the mean household-level relative change, $\bar{G}_{\mathrm{HH}} = \mathbb{E}\left[(X_T - X_0)/X_0\right]$, which gives equal weight to every household trajectory and is inflated by large relative gains of initially small herds; and the relative change in mean herd size, $G_{\mathrm{mean}} = \left(\mathbb{E}[X_T] - \mathbb{E}[X_0]\right)/\mathbb{E}[X_0]$, which describes the aggregate stock. The mean of ratios differs from the ratio of means, so the two quantities must not be used interchangeably.

We also computed the probability of decline $P(X_T < X_0)$ and the probability of quasi-extinction $P(X_T \le 1)$, following [17]. These indicators were estimated from the empirical distribution of the 10,000 simulated final herd sizes.

3.9. Bootstrap and Sensitivity Analysis

To assess the sampling uncertainty of the fitted distribution parameters, we performed non-parametric bootstrap resampling with $B = 5000$ replications, following [30]. For each bootstrap sample, we re-estimated all four distributions and computed 95% percentile confidence intervals for each parameter, in the parameterization of Equations (1)-(4). This procedure quantifies only the sampling uncertainty of the initial herd-size distributions; it does not propagate the uncertainty of the demographic rates, of the environmental noise or of the carrying capacity into the risk indicators, and the resulting intervals are therefore not used as a validation of the simulated risk indicators.

Sensitivity analysis was conducted using a one-at-a-time (OAT) approach, which is computationally efficient and provides a clear ranking of input importance [31]. Each demographic rate mean ($\bar{r}_j^{w}$) was perturbed by +20% and −20% while holding all other rates at their baseline values. For each perturbation, we re-ran the Monte Carlo simulation ($n_{\mathrm{sim}} = 3000$ replications) and computed the relative change in the mean final herd size $\bar{X}_{10}$:

$$\Delta_j^{\pm} = \frac{\bar{X}_{10}^{\pm j} - \bar{X}_{10}^{\mathrm{base}}}{\bar{X}_{10}^{\mathrm{base}}} \times 100\% \tag{11}$$

This allowed us to rank the demographic rates by their influence on herd size

outcomes, identifying the most critical levers for management and policy intervention.

Structural sensitivity. The structural parameters that are not estimated from the survey were examined separately: the full simulation ($N = 10000$) was rerun with every carrying capacity K multiplied by 0.5 and by 1.5, and with every $\sigma_{\text{env},s}$ multiplied by 0.5 and by 1.5, one parameter at a time, and the resulting risk indicators were compared with the baseline.

4. Results

This section presents the empirical findings of the study. We first describe the socio-demographic profile of the surveyed households and the descriptive statistics of herd sizes by species. Next, we report the results of the distribution fitting procedure (Log-Normal, Gamma, Weibull, Inverse Gaussian) with AIC-based model selection and goodness-of-fit assessment. We then present winsorized demographic rates (births, deaths, sales, purchases, own consumption) and the derived net growth rates. Subsequently, we show the outcomes of the Monte Carlo simulations, including mean trajectories, credible intervals, and species-specific carrying capacities. Finally, we provide a comprehensive risk analysis using Value-at-Risk (VaR), Conditional VaR (CVaR), probabilities of decline, and quasi-extinction risks, followed by bootstrap confidence intervals on distributional parameters and the results of the one-at-a-time sensitivity analysis.

4.1. Descriptive Statistics

The surveyed population is characterized by two key socio-demographic variables: sex and level of education. **Table 3** presents the distribution of the 128 agropastoral households across the modalities of each variable, after imputation of the three missing observations on education level to the largest modality code.

The results reveal a strongly male-dominated sample, which reflects the prevailing gender norms in agropastoral communities of the Hauts-Bassins region, where livestock management and household production decisions are traditionally assumed by men. Regarding education, the surveyed households exhibit a structurally low level of formal schooling: nearly half of the respondents have either no formal education at all or have only attended a Quranic school, meaning that their literacy skills in official languages remain largely limited. This pattern is consistent with broader trends in rural Burkina Faso, where access to the formal school system is constrained by geographical remoteness, economic precarity, and the early integration of children into agricultural and pastoral labor [1]. The near-absence of higher education further implies that technology adoption and information diffusion within this population rely primarily on informal channels such as community networks, religious leaders, and peer learning rather than on formal extension services, a finding with direct implications for the design of capacity-building interventions in the livestock sector.

Table 3. Distribution of surveyed households by sex and level of education after imputation of missing values to the largest modality code ($n = 128$, Province du Tuy, Hauts-Bassins, Burkina Faso).

Variable	Modality	*n*	%	Cumul. %
Sex	Male	124	96.88	96.88
	Female	4	3.12	100.00
	Total	128	100.00	
Level of education	None (illiterate)	24	18.75	18.75
	Primary school	33	25.78	44.53
	Secondary school	12	9.38	53.91
	Higher education	0	0.00	53.91
	Quranic school	34	26.56	80.47
	Functional literacy	21	16.41	96.88
	Other	4	3.12	100.00
	Total	128	100.00	

Table 4 summarizes herd size distributions. All species exhibit strong positive skewness (1.25 - 2.32) and high coefficients of variation (50% - 104%), confirming the need for a stochastic framework. Fattening cattle display the highest variability (CV = 103.9%), reflecting heterogeneous investment capacities.

Table 4. Descriptive statistics of livestock herd sizes (herd-owning households only).

Species	*n*	Mean	Med.	SD	Min	Max	CV (%)	Skew	Kurt
Draft Cattle	120	3.41	3.00	1.72	1	10	50.4	1.287	1.599
Fattening Cattle	76	22.46	13.67	23.34	1	96	103.9	1.441	1.577
Sheep	89	10.85	8.00	9.44	1	46	87.0	1.532	2.260
Goats	88	9.49	7.00	8.00	1	40	84.3	1.530	2.379
Hens	112	16.22	14.19	13.67	1	80	84.3	2.323	6.774
Guinea Fowl	31	6.28	5.00	5.19	1	20	82.7	1.248	1.322

SD = standard deviation; CV = coefficient of variation; Med. = median; Skew = skewness; Kurt = excess kurtosis. *n* includes households whose missing herd size was imputed by the sample mean: 2 for fattening cattle, 10 for hens and 9 for guinea fowl (Section 3.2).

The descriptive statistics reveal a livestock system marked by deep structural heterogeneity across both species and households (Table 4). Draft cattle herds are small and relatively homogeneous, reflecting a subsistence-driven traction logic, whereas fattening cattle display extreme variability, indicative of a market-oriented sub-sector dominated by a small number of well-capitalized households.

Small ruminants serve primarily as liquid savings instruments, rapidly mobilized under economic or climatic stress, while poultry widespread but unevenly distributed are embedded in daily consumption and petty trade. Across all species, coefficients of variation exceeding 50% and strongly positive skewness confirm that herd ownership is highly unequal within the surveyed population, with a minority of households holding disproportionately large stocks. This pervasive inequality and the heavy right tails of all distributions provide the empirical justification for the stochastic modeling framework adopted in this study.

4.2. Distribution Fitting

Table 5 reports AIC, BIC, and KS p-values (nominal values and parametric bootstrap values, PB). The Inverse Gaussian provided the best fit for Draft Cattle (AIC = 425.5) and Guinea Fowl (AIC = 174.6); Gamma was optimal for Sheep and Hens; Weibull for Fattening Cattle; Log-Normal for Goats. Figure 2 displays histograms overlaid with the four fitted density curves.

Table 5. Distribution fitting: AIC, BIC, nominal and parametric-bootstrap KS p-values for four candidate distributions. The best-fitting model per species is in bold.

Species	Distribution	AIC	BIC	KS p (nominal)	KS p (PB)
Draft Cattle ($n=120$)	Log-Normal	427.1	432.7	0.000	0.001
	Gamma	435.9	441.5	0.000	0.001
	Weibull	451.6	457.1	0.000	0.001
	Inv. Gauss.	**425.5**	**431.1**	0.000	0.001√
Fatt. Cattle ($n=76$)	Log-Normal	629.0	633.7	0.540	0.128
	Gamma	628.7	633.4	0.481	0.129
	Weibull	**628.6**	**633.2**	0.577	0.154√
	Inv. Gauss.	631.0	635.7	0.127	0.021
Sheep ($n=89$)	Log-Normal	602.6	607.6	0.349	0.039
	Gamma	**600.2**	**605.1**	0.682	0.284√
	Weibull	601.4	606.4	0.540	0.123
	Inv. Gauss.	606.9	611.9	0.040	0.003
Goats ($n=88$)	**Log-Normal**	**565.4**	**570.3**	0.342	0.039√
	Gamma	566.4	571.3	0.442	0.085
	Weibull	568.4	573.4	0.428	0.060
	Inv. Gauss.	566.2	571.2	0.146	0.014
Hens ($n=112$)	Log-Normal	833.5	838.9	0.009	0.001
	Gamma	**832.6**	**838.0**	0.087	0.002√

Continued

	Weibull	837.6	843.1	0.038	0.002
	Inv. Gauss.	842.6	848.1	0.000	0.001
Guinea Fowl ($n = 31$)	Log-Normal	176.1	178.9	0.118	0.001
	Gamma	176.7	179.6	0.164	0.004
	Weibull	177.2	180.1	0.215	0.008
	Inv. Gauss.	**174.6**	**177.4**	0.117	0.007√

$\mathrm{AIC} = -2\hat{\ell} + 2k$; $\mathrm{BIC} = -2\hat{\ell} + k \ln n$; $k = 2$. KS p (nominal): standard KS p-value, not valid when parameters are estimated from the data; reported for reference only. KS p (PB): parametric-bootstrap p-value with re-estimation ($B_{\mathrm{GOF}} = 1000$); $p > 0.05$ indicates no significant departure from the fitted distribution. For Draft Cattle, the nominal KS test rejects all distributions ($p = 0.000$); Inverse Gaussian retained by minimum AIC. A PB p-value of 0.001 means that no bootstrap statistic exceeded the observed one.

The distribution fitting results reveal a heterogeneity in the statistical structure of herd sizes across species (Table 5), but the parametric-bootstrap tests show that an adequate continuous description is achieved for only some of them. The distribution selected by AIC is not rejected for fattening cattle (Weibull, PB $p = 0.154$) and sheep (Gamma, $p = 0.284$). For goats, the selected Log-Normal is rejected at the 5% level ($p = 0.039$), whereas the Gamma ($p = 0.085$) and Weibull ($p = 0.060$) distributions, whose AIC values are within 3.1 units of the minimum, are not. For draft cattle, hens and guinea fowl, all four candidates are rejected ($p \leq 0.008$), although the nominal KS p-values, which ignore parameter estimation, had suggested acceptable fits for hens (Gamma, 0.087) and guinea fowl (0.117 to 0.215). For hens and guinea fowl, part of this misfit is attributable to the 10 and 9 mean-imputed herd sizes (Section 3.2), which create an artificial mass point at the sample mean. For draft cattle, it reflects integer, under-dispersed herd sizes (variance 2.96 for a mean of 3.41) concentrated between one and five animals, which no continuous candidate can represent. For these three species, the selected distributions are therefore pragmatic best approximations by AIC rather than statistically accepted models; the consequences of this misfit are examined with the integer-valued analysis below and in Section 4.8. Species-specific distribution selection nevertheless remains a substantive modeling decision, since the distribution of initial herd sizes conditions the Monte Carlo trajectories and the risk indicators derived from them.

Table 6 reports the zero-truncated count distributions fitted to the observed (non-imputed) integer herd sizes. The ZTNB has the lower AIC for all species except draft cattle, for which the dispersion estimate diverges ($\hat{k} \to \infty$), so that the ZTNB reduces to the ZTP; this is consistent with the under-dispersion of draft cattle herd sizes. The retained count model is not rejected for fattening cattle, sheep, goats and guinea fowl (PB p between 0.449 and 0.883), but it is rejected for draft cattle (ZTP, $p = 0.002$) and hens (ZTNB, $p = 0.007$). Draft cattle herd

sizes, being less dispersed than a Poisson variable, are therefore not well described by any of the continuous or count families considered here.

Table 6. Integer-valued fits of observed herd sizes: zero-truncated Poisson (ZTP) and zero-truncated negative binomial (ZTNB).

Species	n	$\mathrm{AIC}_{\mathrm{ZTP}}$	$\mathrm{AIC}_{\mathrm{ZTNB}}$	$\hat{m}$	$\hat{k}$	KS p (PB)	Retained
Draft Cattle	120	447.7	449.6	3.28	$\to\infty$	0.002	ZTP
Fattening Cattle	74	1935.8	607.5	20.41	0.66	0.550	ZTNB
Sheep	89	981.0	596.8	10.21	1.30	0.449	ZTNB
Goats	88	848.2	564.0	8.96	1.47	0.748	ZTNB
Hens	102	1455.8	765.0	16.12	1.69	0.007	ZTNB
Guinea Fowl	22	145.6	130.8	8.14	4.28	0.883	ZTNB

n: households with an observed (non-imputed) herd size. $\hat{m}$, $\hat{k}$: ZTNB mean and dispersion parameters of Equation (5); for draft cattle $\hat{k}$ diverges and the ZTNB reduces to the ZTP. KS p (PB): parametric-bootstrap KS test on the discrete distribution function of the retained model ($B_{\mathrm{GOF}}=1000$).

4.3. Winsorized Demographic Rates

Table 7 reports winsorized rates by species. Net growth rates range from −0.153 (Guinea Fowl) to +0.083 (Fattening Cattle), revealing sharply contrasting demographic regimes.

Table 7. Winsorized demographic rates by species and flow type. $\bar{r}^{w}$ = winsorized mean; s^{w} = winsorized standard deviation; c = biological ceiling. Net rate $=\bar{r}^{w}_{\mathrm{birth}}+\bar{r}^{w}_{\mathrm{purch}}-\bar{r}^{w}_{\mathrm{sale}}-\bar{r}^{w}_{\mathrm{death}}-\bar{r}^{w}_{\mathrm{cons}}$.

Species	Flow	$\bar{r}^{w}$	s^{w}	c	Net rate
Draft Cattle	Births	0.011	0.059	0.40	−0.083
	Sales	0.126	0.175	0.45	
	Purchases	0.088	0.134	0.35	
	Deaths	0.055	0.097	0.25	
	Own cons.	0.001	0.007	0.08	
Fattening Cattle	Births	0.173	0.162	0.55	+0.083
	Sales	0.074	0.122	0.55	
	Purchases	0.032	0.094	0.35	
	Deaths	0.048	0.069	0.18	
	Own cons.	0.001	0.004	0.05	
Sheep	Births	0.271	0.267	0.90	−0.017
	Sales	0.113	0.164	0.50	

Continued

	Purchases	0.080	0.137	0.35	
	Deaths	0.156	0.120	0.28	
	Own cons.	0.099	0.104	0.25	
	Births	0.240	0.281	0.90	
	Sales	0.192	0.199	0.50	
Goats	Purchases	0.023	0.075	0.35	−0.118
	Deaths	0.122	0.124	0.28	
	Own cons.	0.067	0.084	0.20	
	Births	0.713	0.296	0.85	
	Sales	0.296	0.192	0.45	
Hens	Purchases	0.056	0.101	0.25	−0.008
	Deaths	0.307	0.142	0.38	
	Own cons.	0.174	0.124	0.28	
	Births	0.605	0.301	0.75	
	Sales	0.329	0.199	0.45	
Guinea Fowl	Purchases	0.013	0.020	0.18	−0.153
	Deaths	0.252	0.179	0.38	
	Own cons.	0.189	0.128	0.28	

Ceilings c derived from West African livestock literature (FAO; ILRI).

The winsorized demographic rates reveal sharply contrasting vital dynamics across the six livestock species, with net growth rates ranging from −0.153 for guinea fowl to +0.083 for fattening cattle (Table 7). Fattening cattle stand out as the only species exhibiting a genuinely expansionary demographic regime, driven by a relatively high birth rate that comfortably exceeds the combined pressure of sales, deaths, and own consumption, reflecting the market-oriented intensification logic that characterizes this sub-sector. Draft cattle, by contrast, face a structurally depressed reproduction rate of only 0.011 births per animal per year, far below their sales and mortality rates, which mechanically produces a negative net rate and signals a slow but steady erosion of the draft herd over time. Small ruminants occupy an ambiguous position: their high reproductive potential, with birth rates of 0.271 for sheep and 0.240 for goats, is largely offset by equally elevated mortality and sales rates, leaving sheep near demographic equilibrium and goats in moderate decline, a pattern consistent with their dual role as both productive assets and emergency liquidity reserves. Poultry species face the most acute demographic pressure: hens exhibit the highest birth rate in the

sample (0.713), yet are simultaneously subject to the highest death rate (0.307), suggesting a high-turnover system with considerable biological fragility, while guinea fowl combine a moderate reproductive rate with the heaviest relative mortality and sales burden, resulting in the most negative net rate of the study. Taken together, these results indicate that the demographic vulnerability of most species is not attributable to low fertility alone but to the structural imbalance between reproduction and offtake, a dynamic that conventional deterministic models would systematically underestimate without the stochastic logistic framework applied here.

4.4. Monte Carlo Simulation Results

Table 8 summarizes simulation outputs after 10 years. Figure 3 displays the fan charts showing mean, median, 50% and 90% credible bands, and the carrying capacity K. The mean herd size of fattening cattle increased from 22.3 to 39.0 animals ($G_{\text{mean}} = +74.9\%$; mean household-level change $\bar{G}_{\text{HH}} = +120.3\%$), while that of guinea fowl declined from 6.4 to 2.8 ($G_{\text{mean}} = -56.3\%$; $\bar{G}_{\text{HH}} = -59.6\%$).

Table 8. Monte Carlo simulation summary after $T = 10$ years ($N = 10000$ replications). K = carrying capacity; r_{net} = mean net annual growth rate.

Species	Dist.	K	r_{net}	$\bar{X}_0$	$\bar{X}_{10}$	CI_{95}^{-}	CI_{95}^{+}
Draft Cattle	IG	15	−0.083	3.4	2.0	0.3	6.5
Fatt. Cattle	Weibull	120	+0.083	22.3	39.0	1.8	111.2
Sheep	Gamma	80	−0.017	10.8	14.3	0.5	58.3
Goats	LN	80	−0.118	9.7	6.7	0.2	38.7
Hens	Gamma	150	−0.008	16.3	22.3	0.9	92.6
Guinea Fowl	IG	60	−0.153	6.4	2.8	0.1	16.1

IG = Inverse Gaussian; LN = Log-Normal. CI_{95}^{-}, CI_{95}^{+}: 2.5th and 97.5th percentiles of the X_{10} distribution across simulations.

The Monte Carlo simulation results expose a deeply polarized livestock system in which only fattening cattle follow a genuinely sustainable growth trajectory, while the majority of species face varying degrees of demographic erosion over the ten-year horizon (Table 8, Figure 3). The growth of fattening cattle, which increases its mean herd size by about three quarters (from 22.3 to 39.0 animals, $G_{\text{mean}} = +74.9\%$), reflects a virtuous cycle in which market-oriented management, controlled offtake, and sufficient reproductive performance combine to generate a net surplus, even when biological uncertainty is fully accounted for. Sheep and hens occupy an intermediate position: although both species show a positive mean trajectory, their wide credible intervals, spanning from near-zero to 58.3 and 92.6 animals respectively, signal that a substantial share of households are simultaneously experiencing herd growth and herd col-

lapse, depending on the realization of stochastic demographic shocks. This bimodal household-level outcome is precisely what deterministic models would mask by reporting only the mean. Draft cattle and goats, by contrast, are engaged in a slow but structurally driven decline: the former because of a near-absent reproductive rate relative to sales and mortality pressure, and the latter because of a chronic imbalance between offtake and reproduction that the logistic carrying capacity cannot reverse. Guinea fowl face the most critical trajectory of all, converging toward near-extinction at the household level within a decade, a result driven not by an extreme shock but by the relentless accumulation of moderate annual deficits that compound over time under the stochastic logistic dynamic. Taken as a whole, these projections demonstrate that the long-term viability of smallholder livestock systems in the Hauts-Bassins region is structurally threatened for most species, and that targeted interventions reducing mortality rates and distress sales would be required to reverse the negative demographic regimes identified here.

4.5. Risk Indicators

Table 9 presents the full risk profile. Fattening Cattle shows the most favorable risk profile ($\mathrm{VaR}_{95} = -11.3\%$; $P(\text{decline}) = 8.5\%$). Guinea Fowl and Draft Cattle face critical quasi- extinction risks (47.1% and 28.5%, respectively) and steep VaR_{95} values (−95.0% and −80.0%, i.e. 5th percentiles of the relative change R).

Table 9. Risk indicators for each livestock species over a 10-year Monte Carlo horizon ($N = 10000$).

Species	$\bar{G}_{\mathrm{HH}}$ (%)	G_{mean} (%)	VaR_{95} (%)	CVaR_{95} (%)	$P(\text{dec.})$ (%)	$P(\text{q-ext.})$ (%)
Draft Cattle	−43.0	−41.2	−80.0	−84.3	91.0	28.48
Fatt. Cattle	+120.3	+74.9	−11.3	−28.1	8.5	0.62
Sheep	+42.3	+32.4	−76.9	−83.7	47.5	6.83
Goats	−33.3	−30.9	−91.2	−93.7	80.6	21.54
Hens	+44.2	+36.8	−78.8	−85.0	47.3	3.19
Guinea Fowl	−59.6	−56.3	−95.0	−96.5	92.1	47.05

$\bar{G}_{\mathrm{HH}}$ = mean of household-level relative changes $(X_{10} - X_0)/X_0 \times 100$; G_{mean} = relative change in mean herd size $(\bar{X}_{10} - \bar{X}_0)/\bar{X}_0 \times 100$, computed from the means of Table 8. VaR_{95} = 5th percentile of the relative change R (lower-tail return quantile; negative values are losses). CVaR_{95} = mean of R over trajectories with $R \le \mathrm{VaR}_{95}$, on the same signed scale. $P(\text{dec.}) = P(X_{10} < X_0)$; $P(\text{q-ext.}) = P(X_{10} \le 1)$ (quasi-extinction).

The risk indicators paint a stark picture of asymmetric vulnerability across the six livestock species, with a clear divide between fattening cattle, which exhibit a genuinely resilient risk profile, and the remaining five species, all of which face substantial downside exposure over the ten-year horizon (Table 9). Fattening cattle stand apart not only because of their positive mean growth trajectory, but be-

cause their tail risk is fundamentally different in nature: a VaR_{95} of −11.3% means that only 5% of the simulated household trajectories lose more than 11.3% of their initial herd, and the probability of any decline at all remains below one in ten, making this species the most reliable store of livestock wealth in the surveyed system. Guinea fowl and draft cattle, at the opposite extreme, face what can only be described as a structural viability crisis: the probability that a guinea fowl herd is reduced to near-extinction within a decade exceeds one in two, while nearly three in ten draft cattle herds face the same fate, implying that without corrective intervention, both species will progressively disappear from a significant share of smallholder portfolios. Goats occupy a particularly precarious intermediate position, combining an 80.6% probability of decline with a $CVaR_{95}$ of −93.7%, which means that, averaged over the worst 5% of trajectories, 93.7% of the initial herd is lost, leaving households without the liquid savings buffer that small ruminants are traditionally expected to provide. Sheep and hens, despite displaying positive mean growth ($\bar{G}_{HH} = +42.3\%$ and +44.2%; $G_{mean} = +32.4\%$ and +36.8%), carry substantial hidden risk: their probabilities of decline hover around 47% and their $CVaR_{95}$ values are at or below −83.7%, revealing that the optimistic mean trajectory masks a near-even chance of herd contraction at the household level. Collectively, these results demonstrate that conventional mean-based assessments would dramatically understate the risk exposure of agropastoral households in the Hauts-Bassins region, and that VaR and CVaR metrics grounded in stochastic simulation provide a fundamentally more actionable basis for the design of livestock insurance schemes, emergency credit facilities, and veterinary support programs.

4.6. Bootstrap Confidence Intervals

Table 10 presents the 95% bootstrap intervals ($B = 5000$) for all distributional parameters. All parameters are given in the parameterization of Equations (1)-(4). These intervals describe the sampling uncertainty of the initial herd-size fits only.

Table 10. Bootstrap confidence intervals ($B = 5000$) on the parameters of the four candidate distributions, in the parameterization of Equations (1)-(4): Log-Normal (μ, σ), Gamma (α, β), Weibull (c, λ) and Inverse Gaussian (μ, λ).

Panel A. Log-Normal and Gamma

Species	Best dist.	$\hat{\mu}_{LN}$ [CI95]	$\hat{\sigma}_{LN}$ [CI95]	$\hat{\alpha}_G$ [CI95]	$\hat{\beta}_G$ [CI95]
Draft Cattle	InvGauss	1.115 [1.035; 1.199]	0.462 [0.412; 0.509]	4.668 [3.882; 5.876]	0.730 [0.553; 0.920]
Fattening Cattle	Weibull	2.491 [2.215; 2.769]	1.224 [1.066; 1.356]	0.937 [0.790; 1.183]	23.971 [16.887; 31.251]
Sheep	Gamma	1.996 [1.796; 2.193]	0.950 [0.809; 1.068]	1.430 [1.167; 1.871]	7.592 [5.372; 9.993]
Goats	LogNorm	1.900 [1.713; 2.076]	0.878 [0.763; 0.979]	1.576 [1.308; 2.052]	6.021 [4.237; 7.833]
Hens	Gamma	2.484 [2.328; 2.633]	0.819 [0.693; 0.937]	1.804 [1.437; 2.419]	8.995 [6.135; 12.162]
Guinea Fowl	InvGauss	1.481 [1.176; 1.788]	0.883 [0.728; 0.997]	1.550 [1.205; 2.345]	4.052 [2.356; 5.881]

Continued

Panel B. Weibull and Inverse Gaussian					
Species	Best dist.	$\hat{c}_W$ [CI95]	$\hat{\lambda}_W$ [CI95]	$\hat{\mu}_{IG}$ [CI95]	$\hat{\lambda}_{IG}$ [CI95]
Draft Cattle	InvGauss	2.133 [1.924; 2.457]	3.869 [3.528; 4.219]	3.408 [3.108; 3.733]	14.455 [11.941; 18.045]
Fattening Cattle	Weibull	0.945 [0.843; 1.104]	21.872 [16.905; 27.625]	22.456 [17.381; 27.877]	7.843 [5.685; 11.877]
Sheep	Gamma	1.211 [1.071; 1.413]	11.603 [9.588; 13.874]	10.854 [8.966; 12.865]	7.772 [5.706; 11.855]
Goats	LogNorm	1.267 [1.130; 1.470]	10.269 [8.541; 12.205]	9.489 [7.897; 11.193]	8.587 [6.426; 12.501]
Hens	Gamma	1.329 [1.172; 1.603]	17.758 [15.164; 20.524]	16.223 [13.944; 18.882]	16.489 [11.975; 25.204]
Guinea Fowl	InvGauss	1.272 [1.073; 1.683]	6.798 [4.950; 9.004]	6.280 [4.589; 8.150]	5.927 [4.317; 9.708]

Values shown as maximum likelihood point estimate [lower 2.5th; upper 97.5th percentile of the bootstrap distribution]. LN = Log-Normal; G = Gamma; W = Weibull; IG = Inverse Gaussian. $\hat{\mu}_{IG}$ is the mean of the Inverse Gaussian (Equation 4); with scipy.stats.invgauss(m,scale), $\mu = m \cdot \text{scale}$ and $\lambda = \text{scale}$.

The bootstrap intervals indicate that the parameters of the initial herd-size distributions are estimated with reasonable precision for most species (Table 10). The Log-Normal location parameter $\hat{\mu}_{LN}$ has interval widths below 0.4 log-units for draft cattle, sheep, goats and hens, and wider intervals for fattening cattle (0.55) and guinea fowl (0.61). The widest relative uncertainty is observed for the Gamma scale parameter $\hat{\beta}_G$ of fattening cattle (16.89 to 31.25), reflecting the high empirical variability of this category and the comparatively small number of herd-owning households ($n = 76$), and for all parameters of guinea fowl, the smallest sub-sample ($n = 31$). These samples include the mean-imputed herd sizes described in Section 3.2, which tend to understate the true sampling variability. These intervals, however, quantify only the sampling uncertainty of the initial herd-size fits. They do not account for the uncertainty in the demographic rates, the environmental noise or the carrying capacities, which jointly drive the simulated trajectories, and they therefore cannot be interpreted as a validation of the risk indicators of Table 9. The sensitivity of these indicators to the demographic rates, to K, to $\sigma_{env,s}$ and to the specification of the demographic process is examined separately in Table 11 and Section 4.8.

4.7. Sensitivity Analysis

Figure 4 shows the tornado charts. Birth rates are the dominant drivers for small ruminants and poultry (Hens: +64.9%/−55.9%; Guinea Fowl: +82.6%/−47.3%). For Draft Cattle, purchases and sales dominate (±13%), reflecting the primacy of market transactions over natural reproduction. Death rates rank second or third across all species. Full OAT results are in Table 11.

The one-at-a-time sensitivity analysis reveals that the dominant driver of herd size outcomes is not the same across species, pointing to fundamentally different leverage points for management and policy intervention depending on the production system considered (Table 11, Figure 4). For poultry and small ruminants,

the birth rate is overwhelmingly the most influential parameter: a 20% increase in the reproductive rate of guinea fowl amplifies the mean final herd size by 82.6%, while the symmetric reduction produces a contraction of 47.3%, an asymmetry that reflects the non-linear logistic structure of the model and indicates that reproductive gains yield disproportionately large returns when a species is operating well below its carrying capacity. For sheep and goats, death rates emerge as nearly co-dominant with birth rates in their influence on herd trajectories, suggesting that for these species the simultaneous action of veterinary care and improved reproductive management would be required to achieve meaningful demographic improvements, as gains on one front would be partially neutralized by losses on the other. Draft cattle constitute a structurally distinct case: the near-absence of natural reproduction makes the birth rate almost irrelevant as a leverage point, while purchases and sales collectively determine more than a quarter of the variation in final herd size, confirming that the demographic trajectory of this species is governed by market access and transaction costs rather than by biological productivity. Fattening cattle, the only species with a positive net growth rate, display a more balanced sensitivity profile in which births, sales, and deaths contribute comparably to outcome variability, suggesting that their favorable trajectory is robust to moderate shocks on any single rate but could be destabilized by the simultaneous deterioration of several drivers. Collectively, these findings provide a rigorous empirical basis for prioritizing interventions: for poultry and guinea fowl, reproductive enhancement programs offer the highest marginal return; for small ruminants, mortality reduction through subsidized veterinary access is equally critical; and for draft cattle, facilitating market access and reducing distress sales represent the most actionable levers available to policymakers in the Hauts-Bassins region.

Table 11. One-at-a-time (OAT) sensitivity analysis: relative change in mean final herd size $\bar{X}_{10}$ following a ±20% perturbation of each demographic rate ($n_{\text{sim}} = 3000$; $T = 10$ years).

Species	Rate	+20% (%)	−20% (%)
Draft Cattle	Births	+3.3	+0.9
	Sales	−12.8	+15.9
	Purchases	+13.0	−8.8
	Deaths	−6.9	+6.2
	Own cons.	+1.5	−0.6
Fatt. Cattle	Births	+9.9	−17.3
	Sales	−8.9	+1.0
	Purchases	−0.3	−5.5
	Deaths	−8.3	+1.4
	Own cons.	−2.9	−5.1

Continued

	Births	+35.1	−24.7
	Sales	−13.7	+12.1
Sheep	Purchases	+3.8	−8.3
	Deaths	−14.0	+18.1
	Own cons.	−6.6	+11.6
	Births	+27.5	−26.9
	Sales	−18.6	+21.3
Goats	Purchases	−0.1	−1.6
	Deaths	−12.8	+14.5
	Own cons.	−5.7	+9.5
	Births	+64.9	−55.9
	Sales	−27.4	+30.9
Hens	Purchases	+0.8	−10.6
	Deaths	−29.9	+34.9
	Own cons.	−19.2	+19.0
	Births	+82.6	−47.3
	Sales	−27.7	+57.3
Guinea Fowl	Purchases	+6.9	+2.5
	Deaths	−19.5	+44.8
	Own cons.	−20.6	+28.9

Baseline $\bar{X}_{10}^{\text{base}}$: Draft Cattle = 1.99; Fatt. Cattle = 40.04; Sheep = 14.38; Goats = 6.78; Hens = 22.97; Guinea Fowl = 2.67. Asymmetric responses reflect the non-linear logistic structure of the stochastic model.

4.8. Robustness Checks

Table 12 reports the probabilities of decline and of quasi-extinction when the carrying capacities and the environmental-noise parameters are varied, and Table 13 compares the baseline model with the integer-valued stock-constrained event model (Section 3.7). Varying K or $\sigma_{\text{env},s}$ by ±50% leaves the probabilities of decline and of quasi-extinction largely unchanged (Table 12), and the ranking of species by quasi-extinction risk is the same in all scenarios. Changes in $\sigma_{\text{env},s}$ modify the probability of quasi-extinction by less than one percentage point for every species. The largest effects concern K : for draft cattle, the probability of quasi-extinction is 22.4% with $0.5K$ and 31.1% with $1.5K$ (28.7% at baseline), and for fattening cattle the probability of decline rises from 8.6% to 15.0% with

$0.5K$. For categories with a negative mean net rate, a smaller K attenuates the decline because the factor $(1-X_t/K)$ multiplies $r_{\text{net},t}$ in Equation (7).

Table 12. Structural sensitivity of the risk indicators to the carrying capacity K and to the environmental noise $\sigma_{\text{env},s}$ ($N=10000$; $T=10$ years).

Species	Baseline	$0.5K$	$1.5K$	$0.5\sigma_{\text{env}}$	$1.5\sigma_{\text{env}}$
Panel A. Probability of decline $P(X_{10}<X_0)$ (%)					
Draft Cattle	91.43	86.59	91.51	91.43	89.77
Fattening Cattle	8.60	15.04	8.19	7.20	9.16
Sheep	47.52	46.52	47.54	47.62	46.86
Goats	80.41	79.01	81.22	81.84	80.11
Hens	47.57	46.84	47.43	47.21	46.75
Guinea Fowl	92.31	90.26	92.81	93.23	91.06
Panel B. Probability of quasi-extinction $P(X_{10}\le 1)$ (%)					
Draft Cattle	28.70	22.36	31.12	28.31	29.17
Fattening Cattle	0.58	0.53	0.61	0.45	0.69
Sheep	6.48	6.10	6.44	6.76	6.62
Goats	21.83	20.93	22.50	22.09	22.08
Hens	3.10	3.10	2.93	3.10	3.82
Guinea Fowl	47.51	44.61	49.22	47.67	47.54

One parameter varied at a time; all other inputs at baseline values (Table 2 and Table 7); initial herd sizes are identical across scenarios. Baseline: re-run of the baseline model with the same inputs; differences with Table 9 (at most 0.5 percentage point) reflect Monte Carlo error.

In contrast, the integer-valued stock-constrained event model produces materially different results (Table 13). The probability of quasi-extinction is higher for every species: 70.3% versus 28.7% for draft cattle, 61.7% versus 21.8% for goats, 50.7% versus 47.5% for guinea fowl, 36.5% versus 6.5% for sheep, 19.0% versus 3.1% for hens and 8.8% versus 0.6% for fattening cattle. The relative change in mean herd size remains positive for fattening cattle (+13.0% versus +74.3%), is close to zero for hens (+0.6% versus +37.0%) and becomes negative for sheep (−42.3% versus +32.8%). Because at least 5% of the event-model trajectories reach zero for every species, VaR_{95} and CVaR_{95} equal −100%. The household-level demographic rates are mostly positively correlated (56 of the 60 species-flow pairs; Spearman coefficients from −0.16 to 0.72), most strongly for guinea fowl (0.21 to 0.71), so that flows tend to co-occur within households. These comparisons show that the independence and continuous-state approximations of the baseline model are not innocuous. They leave unchanged the contrast between fattening cattle,

the least exposed category, and draft cattle, goats and guinea fowl, the most exposed ones, but they markedly affect the magnitude of the risk indicators and reverse the projected growth of sheep. Part of the difference arises because the event model represents demographic stochasticity in small integer herds, in which zero is absorbing, and because its initial sizes are drawn from the observed (non-imputed) herd sizes. The baseline risk indicators must therefore be read as conditional on the baseline specification rather than as robust point predictions.

Table 13. Baseline stochastic logistic model versus the integer-valued stock-constrained event model (ISEM) ($N = 10000$; $T = 10$ years).

Species	Model	$\bar{G}_{HH}$ (%)	G_{mean} (%)	VaR_{95} (%)	$CVaR_{95}$ (%)	$P(\text{dec.})$ (%)	$P(\text{q-ext.})$ (%)
Draft Cattle	Baseline	−43.2	−41.4	−80.0	−84.2	91.4	28.70
	ISEM	−65.0	−66.1	−100.0	−100.0	86.0	70.26
Fatt. Cattle	Baseline	+120.0	+74.3	−12.3	−27.2	8.6	0.58
	ISEM	+61.9	+13.0	−100.0	−100.0	36.5	8.77
Sheep	Baseline	+43.3	+32.8	−76.5	−83.4	47.5	6.48
	ISEM	−26.3	−42.3	−100.0	−100.0	74.7	36.53
Goats	Baseline	−32.8	−31.0	−90.9	−93.5	80.4	21.83
	ISEM	−68.7	−73.0	−100.0	−100.0	90.7	61.68
Hens	Baseline	+42.8	+37.0	−78.3	−85.2	47.6	3.10
	ISEM	+41.8	+0.6	−100.0	−100.0	53.8	19.00
Guinea Fowl	Baseline	−60.1	−56.2	−94.8	−96.4	92.3	47.51
	ISEM	−55.4	−61.7	−100.0	−100.0	84.6	50.67

Indicators defined as in Table 9. Baseline: re-run of the baseline model (see Table 12). ISEM: integer initial sizes from the retained zero-truncated distribution (Table 6), jointly resampled household rate vectors and stock-constrained events (Equation 8).

Figure 2 provides a visual confirmation of the distributional heterogeneity quantified in Table 5: across all six species, the empirical histograms share the same fundamental shape, being unimodal, right-skewed, and concentrated near small herd sizes, yet the best-fitting theoretical curve differs systematically from one species to another, illustrating that this common shape is produced by distinct underlying demographic processes. For fattening cattle and sheep, for which the selected distribution is not rejected by the parametric-bootstrap test, the fitted curves track the histogram closely throughout the entire support, including the right tail, which is the region most consequential for risk assessment since it governs the probability of encountering unusually large herds that anchor the upper bound of the simulated trajectories. For draft cattle and guinea fowl, the Inverse Gaussian curve comes closest, among the four candidates, to reproducing the sharp initial peak and the rapid decay of the distribution, reflecting the biological

reality that these species are predominantly held in very small numbers per household with only a thin tail of larger owners. The persistent gap between any fitted curve and the draft cattle histogram, visible across all four distributions, provides intuitive support for the analytical finding that no standard continuous distribution can fully represent a herd size variable that is effectively discrete and bounded between one and ten animals, reinforcing the call for discrete distribution alternatives in future work.

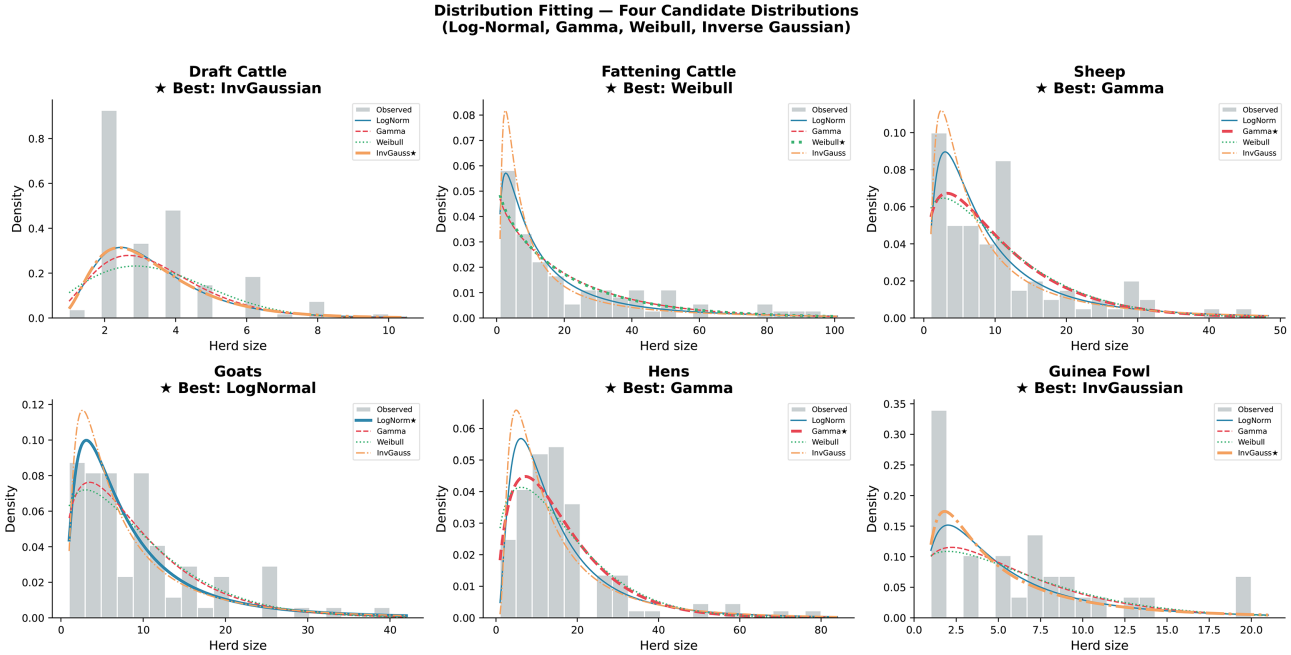

Figure 2. Distribution fitting for six livestock species. Grey bars: observed frequency histograms. Fitted density curves: Log-Normal (blue, solid), Gamma (red, dashed), Weibull (green, dotted), Inverse Gaussian (orange, dash-dot). The best-fitting distribution (lowest AIC) is marked with $\star$. For Draft Cattle, all KS tests reject H_0 ($p = 0.000$); Inverse Gaussian retained by minimum AIC.

Figure 3 translates the summary statistics of Table 8 into a dynamic visual narrative that reveals features of the herd trajectories that point estimates alone cannot convey. The most striking observation is the progressive divergence between the mean and the median trajectories for most species, a signature of distributional skewness that intensifies over time: as the simulation horizon extends, a minority of households experience sustained herd growth while the majority converges toward very small or null herds, pulling the mean upward while the median stagnates or declines. For fattening cattle, the fan chart conveys genuine optimism: the 50% credible band remains well above the initial herd size throughout the entire horizon, and even the lower bound of the 90% interval stays in a range consistent with economically meaningful herd sizes, confirming that this species offers a robust investment opportunity even under adverse stochastic conditions. For guinea fowl and draft cattle, the fan charts tell the opposite story: the 90% credible interval collapses toward zero well before year ten, and the individual grey paths show that extinction trajectories are not rare outliers but a structurally re-

current outcome, occurring across a broad range of random realizations. The carrying capacity line K serves as a meaningful upper reference: for most species, the upper credible band approaches but rarely breaches K, validating the biological plausibility of the logistic ceiling embedded in the model and ensuring that the simulated growth is constrained within ecologically defensible bounds.

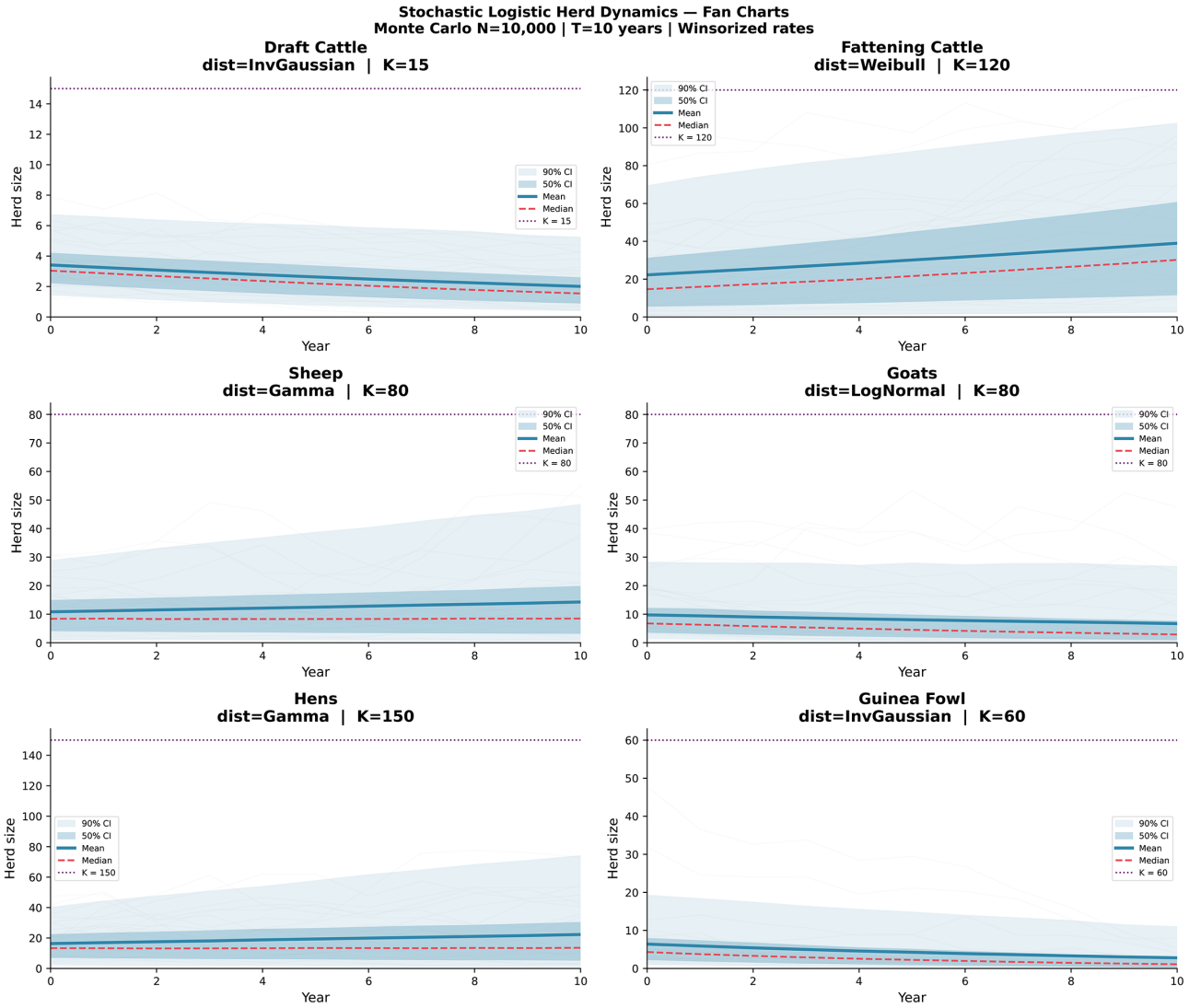

Figure 3. Fan charts of stochastic herd trajectories over $T = 10$ years ($N = 10000$ Monte Carlo replications). Light shading: 90% credible interval. Dark shading: 50% credible interval. Solid blue line: mean; dashed red line: median. Dotted horizontal line: carrying capacity K. Grey lines: 25 randomly selected individual paths.

Figure 4 synthesizes the sensitivity analysis into a visually immediate ranking of demographic drivers across species, making two structural patterns instantly legible that would remain obscured in a numerical table alone. The first pattern is the species-specific dominance hierarchy: for poultry and small ruminants, the birth rate bar dwarfs all others, towering above the remaining drivers and signaling that reproductive performance is the single critical bottleneck in these systems, whereas

for draft cattle the bars for purchases and sales are the widest, visually encoding the market-dependency of this species and the irrelevance of reproductive dynamics as a management lever. The second pattern is the systematic asymmetry between the green and red bars across nearly all species and rates: negative shocks consistently produce larger absolute impacts than equivalent positive shocks, a hallmark of the non-linear logistic growth structure in which a population already operating below its carrying capacity can absorb gains more easily than it can resist losses, implying that risk mitigation strategies will generally be more effective than equivalent growth-promotion efforts of the same magnitude. The compression of all bars toward near-zero for own consumption across all species further confirms that this flow, while present, constitutes a negligible lever for herd management, a finding that simplifies the intervention landscape by allowing policymakers to focus exclusively on births, deaths, and market transactions as the actionable drivers of livestock demographic outcomes in the Hauts-Bassins region.

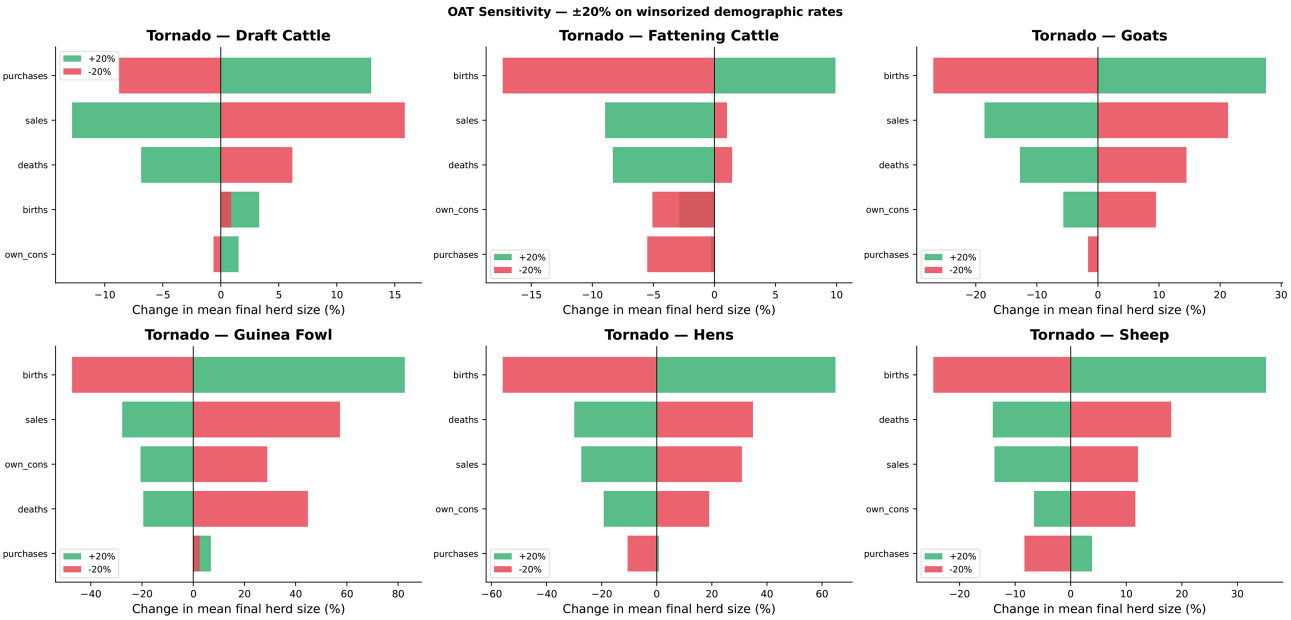

Figure 4. Tornado charts from the one-at-a-time (OAT) sensitivity analysis for all six livestock species. Green bars: relative change in mean final herd size $\bar{X}_{10}$ following a +20% perturbation of each demographic rate mean. Red bars: relative change following a −20% perturbation. Rates ranked by absolute impact (most influential at top). $n_{\text{sim}} = 3000$; $T = 10$ years.

5. Discussion

5.1. Heterogeneous Herd Dynamics and Their Structural Drivers

The Monte Carlo simulation results reveal a livestock system in deep structural tension, where only one species out of six follows a genuinely sustainable demographic trajectory over a ten-year horizon. This finding aligns with the broader literature on smallholder agropastoral systems in sub-Saharan Africa, which consistently documents the coexistence of growth and erosion dynamics within the same household portfolio, depending on species, market integration, and access

to veterinary services [2] [4]. The positive trajectory of fattening cattle, which increases its mean herd size by about three quarters, from 22.3 to 39.0 animals, reflects a virtuous cycle in which market-oriented management, controlled offtake, and sufficient reproductive performance combine to generate a net surplus even when biological uncertainty is fully accounted for. This market orientation is consistent with the findings of [32] in the nearby province of Solenzo, who document that access to output markets and the availability of production-enhancing inputs are the principal explanatory factors of agricultural performance in the same agroclimatic zone of Burkina Faso, a mechanism that appears to extend from crop to livestock production systems. The structural heterogeneity observed across species also resonates with the multi-level modeling framework developed by [13] for agro-ecosystems in semi-arid Burkina Faso, which demonstrates that species-specific demographic regimes respond to qualitatively different combinations of climatic, institutional, and market drivers.

5.2. Structural Vulnerability of Draft Cattle and Guinea Fowl

The near-critical demographic situation of draft cattle and guinea fowl reflects two qualitatively different forms of structural vulnerability. For draft cattle, the vulnerability is rooted in the composition of the category (Section 3.3): a crude birth rate of only 0.011 births per head of the category per year is insufficient to compensate even moderate sales and mortality rates, producing a negative net demographic balance that no stochastic variability can reverse at the population level [2]. This low reproductive rate is not a biological accident but a management outcome: draft cattle are predominantly male animals used for traction, and households have little incentive to invest in reproductive management for a species whose primary function is mechanical rather than biological. The progressive displacement of animal traction by motorized equipment in more accessible zones of the Hauts-Bassins region further reduces the demand for draft cattle and accelerates the erosion of herd sizes, a transition that would deserve specific investigation. For guinea fowl, the vulnerability is of a different nature: reproductive potential is not negligible (birth rate of 0.605), but it is systematically outpaced by a combination of high mortality (0.252) and heavy sales pressure (0.329) that together absorb nearly the entire reproductive surplus every year. This pattern is characteristic of extensive free-range poultry systems in the Sudanian zone, where predation, disease outbreaks, and the absence of veterinary coverage generate structural mortality rates that cannot be compensated by natural reproduction alone [3]. The influence of climate variability on disease occurrence in Burkina Faso, documented by [3], further suggests that mortality rates for guinea fowl are likely to increase under projected climate scenarios, making the already precarious demographic balance of this species even more fragile in the medium term.

5.3. Hidden Risk of Apparently Growing Species

One of the most policy-relevant findings of this study is the demonstration that

positive mean growth trajectories can coexist with substantial probabilities of household-level herd decline, a paradox that only the stochastic modeling framework can reveal [17] [29]. Sheep and hens both display positive mean household-level growth ($\bar{G}_{HH}$ = +42.3% and +44.2% respectively; relative change in mean herd size +32.4% and +36.8%), yet both carry a near-even probability of decline at the household level (47.5% and 47.3%), and their $CVaR_{95}$ values are at or below −83.7%, meaning that over the worst 5% of trajectories more than four fifths of the initial herd is lost on average. This divergence between the mean and the median trajectory, which widens over time as shown in the fan charts, is a direct consequence of the log-normal-type skewness of the herd size distribution: a minority of growing households pulls the mean upward while the majority experiences stagnation or contraction [8]. Deterministic models, which report only the mean, would therefore convey a systematically overoptimistic picture of these species and lead policymakers to underallocate risk management resources to households that are, in practice, highly exposed [17]. This finding resonates with the review of [5], who found that farm household models are generally weak on risk analysis and called for approaches able to evaluate climate impacts and adaptive management under uncertainty. The stochastic logistic growth framework applied here directly addresses this limitation by propagating demographic uncertainty through the entire simulation horizon, in line with stochastic herd models used to analyse the post-drought recovery of Sahelian cattle [2]. The projected growth of sheep and hens is, however, not robust to the specification of the demographic process: under the integer-valued stock-constrained event model, the mean herd size of sheep declines and that of hens remains stable, while their probabilities of household-level decline increase to 74.7% and 53.8% (**Table 13**). What is robust across specifications is the high probability of household-level decline of these species, not their mean growth.

5.4. Distributional Heterogeneity and Modeling Implications

The rejection of a single universal distribution across all six species is not a statistical inconvenience but a substantively meaningful result that carries direct implications for the design of livestock risk models [24]. The lower AIC of the Inverse Gaussian for draft cattle and guinea fowl is only a relative advantage, since all continuous candidates are rejected by the parametric-bootstrap test for these species (**Table 5**). It is nonetheless consistent with herds that are small and tightly clustered near the lower end of the ownership distribution, with a right tail generated by a small number of larger-scale owners [2]. This ownership structure is characteristic of species that function as entry-level assets for resource-poor households, which accumulate them incrementally in small numbers, a pattern consistent with the herd-size distributions observed in this survey. The failure of all standard continuous distributions to adequately fit draft cattle herd sizes further suggests that the underlying ownership variable is effectively discrete and bounded, a property that future modeling efforts should address through the ex-

plicit use of discrete distributions such as the negative binomial or the zero-inflated Poisson [7]; the integer-valued analysis reported in Section 4.8, based on zero-truncated count distributions (zero inflation being irrelevant when only herd owners are modeled), shows that the zero-truncated negative binomial is adequate for fattening cattle, sheep, goats and guinea fowl, whereas the under-dispersed herd sizes of draft cattle call for other families, such as under-dispersed count models. The species-specific selection of best-fitting distributions adopted in this study is consistent with [9], who showed that the choice of distribution matters for summarising caprine age-at-death profiles.

5.5. Sensitivity Analysis and Policy Leverage Points

The one-at-a-time sensitivity analysis produces a clear and actionable hierarchy of demographic drivers that differs fundamentally across the species groups identified in this study [31]. For poultry and small ruminants, the dominant sensitivity to birth rates means that reproductive enhancement programs, including selective breeding, improved nutritional support during gestation, and access to reproductive health services, would generate the highest marginal return per unit of policy investment. For goats and sheep, the near co-dominance of birth and death rates in the sensitivity rankings implies that single-lever interventions targeting only reproduction or only mortality will have limited effectiveness, and that an integrated approach combining veterinary support with reproductive management is required to shift the demographic balance of these species from negative to positive [14]. For draft cattle, the dominance of market transactions over biological parameters points to a fundamentally different policy design: interventions should focus on reducing the frequency and magnitude of distress sales by strengthening household liquidity through savings and credit instruments, and on improving the terms of trade for draft animals [16] [32]. These differentiated recommendations are consistent with the multi-dimensional approach to agricultural development advocated by [32] in the context of cotton production in Burkina Faso, where the authors demonstrate that sustainable productivity gains require simultaneous action on market access, input availability, and risk management, rather than single-lever technical interventions. The asymmetry between the effects of positive and negative rate shocks, systematically observed across all species, further implies that risk mitigation strategies will generally be more effective than equivalent growth-promotion efforts of the same magnitude, a result consistent with the use of robustness and adaptability criteria in viability analyses of mixed herds [18].

5.6. Limitations and Directions for Future Research

Several limitations of this study should be acknowledged in order to properly bound the scope of its conclusions [31]. First, the cross-sectional nature of the household survey prevents direct empirical validation of the ten-year projections: the simulated trajectories represent probabilistic scenarios conditioned on the demographic rates observed at a single point in time, not longitudinal forecasts [5].

Collecting panel data over multiple years would allow for the direct calibration and validation of the stochastic model against observed herd dynamics, substantially strengthening the inferential basis of the risk estimates [20]. Second, although demographic rates vary randomly from one year to the next in the simulation, their distributions are assumed stationary and were estimated from a single recall period, whereas in reality they are subject to trends and serially correlated variability driven by rainfall fluctuations, epidemic episodes, and market price cycles [3] [4]. Incorporating climate-driven, serially correlated rates estimated from multi-year data would introduce an additional layer of environmental realism into the model and would likely increase the width of the credible intervals reported here. Third, the carrying capacities and the environmental-noise parameters were fixed by assumption rather than estimated (**Table 2**). Their influence on the risk indicators proved small within the explored range (**Table 12**), but the indicators remain conditional on these inputs and on the point estimates of the demographic rates, because a full propagation of all sources of uncertainty (for instance by a nested bootstrap of households, rates and structural parameters) was not performed. Fourth, the households were selected purposively among members of producer groups, with deliberate inclusion of large cattle owners, so that the results describe the surveyed farms and cannot be extrapolated to all agropastoral households of the province without caution; annual flows were collected retrospectively and may be affected by recall error; missing herd sizes and flows were imputed by sample means, which understates variability and, for hens and guinea fowl, creates artificial mass points in the herd-size distributions; and the birth rate is a crude rate per head of functional categories whose sex-age composition is assumed stationary (Section 3.3). Fifth, the baseline model treats herd size as continuous and the demographic rates as independent; the comparison with the integer-valued stock-constrained event model (**Table 13**) shows that these approximations substantially affect the magnitude of the risk indicators, in particular the quasi-extinction probabilities and the projected growth of sheep and hens, while preserving the contrast between the least and the most exposed categories. A model combining integer dynamics, jointly distributed rates and explicit uncertainty propagation would be a natural extension. Sixth, the moderate sample size for guinea fowl ($n = 31$, of which 22 with an observed herd size) limits the precision of the distributional estimates for this species, as reflected in the wider bootstrap confidence intervals [30], and future surveys should oversample minority species to improve the statistical power of the analysis. Finally, the spatial dimension of herd dynamics, including seasonal transhumance, cross-village trading networks, and localized disease outbreaks, was not captured in the current model and represents a promising avenue for extension through spatially explicit agent-based modeling frameworks [15].

6. Conclusions

This study developed a stochastic logistic herd dynamics framework for six live-

stock species in 128 agropastoral households of the Province du Tuy, Hauts-Bassins region, Burkina Faso, integrating four candidate distributional families, Monte Carlo simulation with $N = 10000$ replications, and a comprehensive risk assessment toolkit comprising Value-at-Risk, Conditional VaR, extinction probabilities, bootstrap confidence intervals, and one-at-a-time sensitivity analysis. The methodological contribution of this work lies in its demonstration that the combination of species-specific distribution selection, winsorized demographic rate estimation, and stochastic logistic growth modeling can produce household-level risk estimates that are both statistically rigorous and operationally interpretable for livestock development practitioners [29] [31].

The empirical findings reveal a livestock system characterized by deep structural heterogeneity across species and households. Fattening cattle stand as the only species exhibiting a genuinely sustainable demographic trajectory, driven by a market-oriented production logic that generates a positive net growth rate robust to stochastic shocks. Draft cattle and guinea fowl, by contrast, face critical quasi-extinction risks at the household level within a decade, resulting from structurally negative demographic balances that no level of stochastic variability can reverse in the absence of targeted interventions [2] [3]. Sheep, goats, and hens occupy an ambiguous intermediate position where positive mean trajectories coexist with near-even probabilities of household-level herd decline, a paradox that deterministic models would systematically conceal and that only the stochastic framework adopted here can reveal [17]. These conclusions are conditional on the assumed carrying capacities and environmental noise, to which they proved insensitive within ±50%, and on the stationarity of the demographic rates. Under an integer-valued, stock-constrained alternative model, quasi-extinction risks are higher for all species and the projected growth of sheep and hens is not reproduced, whereas fattening cattle remain the least exposed category and draft cattle, goats and guinea fowl the most exposed ones (Section 4.8).

The sensitivity analysis provides a clear and actionable hierarchy of intervention priorities: reproductive enhancement for poultry and small ruminants, integrated veterinary and reproductive support for goats and sheep, and market access improvement combined with distress sale reduction for draft cattle. These recommendations are differentiated by species and grounded in the quantitative ranking of demographic drivers, offering a more precise basis for resource allocation than the qualitative prescriptions that dominate the current policy discourse on smallholder livestock development in the Sahel [1] [4] [32].

Beyond its immediate empirical findings, this study makes a broader methodological argument: the distributional heterogeneity observed across species, the systematic divergence between mean and median trajectories, and the species-specific sensitivity hierarchies all demonstrate that probabilistic stochastic frameworks are not a technical luxury but a substantive necessity for any credible assessment of livestock system viability in risk-prone agropastoral environments [2] [4]. The widespread reliance on deterministic mean-based models in the livestock

development literature therefore represents a structural gap that this study contributes to closing.

Several directions for future research emerge naturally from the present work. The extension of the framework to panel data settings would enable the direct empirical validation of the simulated trajectories and the calibration of time-varying demographic rates that reflect the inter-annual climate and market variability characteristic of the Sudanian zone [13] [23]. The integration of spatially explicit dynamics, including seasonal transhumance routes, cross-village trading networks, and spatially heterogeneous disease pressure, would further increase the realism of the projections and their relevance for territorial planning [14] [15]. Finally, the explicit modeling of household wealth heterogeneity and its interaction with demographic rates would allow the framework to capture the within-species variance in trajectories that the current aggregate approach can only partially represent [5] [32]. The probabilistic toolkit developed here is deliberately designed to be transferable to other agropastoral systems in West Africa and beyond, wherever primary household survey data on livestock demographics are available and where the design of evidence-based risk management policies demands a rigorous quantification of downside exposure at the household level.

Author Contributions

Daouda Traoré: conceptualization, writing—original draft (entire manuscript). **Malik Garané**: validation of the research problem. **Joël Dabiré**: literature review. **Drissa Hié**: validation of the study population and of the data sources. **Vincent Dah**: review of the Discussion and Conclusion sections. All authors read and approved the final manuscript.

Conflicts of Interest

We declare that we have no conflict of interest.

References

[1] FAO (2018) Africa Sustainable Livestock 2050—Livestock Production Systems Spotlight: Cattle and Poultry Sectors in Burkina Faso. Food and Agriculture Organization of the United Nations. https://fao.org/3/i8492en/I8492EN.pdf

[2] Lesnoff, M., Corniaux, C. and Hiernaux, P. (2012) Sensitivity Analysis of the Recovery Dynamics of a Cattle Population Following Drought in the Sahel Region. *Ecological Modelling*, **232**, 28-39. https://doi.org/10.1016/j.ecolmodel.2012.02.018

[3] Sanou, C.L., Agodzo, S.K., Balima, L.H., Bessah, E., Antwi-Agyei, P. and Traoré, K. (2025) Influence of Climate Change on Livestock Diseases Occurrence in Burkina Faso, West Africa. *International Journal of Biometeorology*, **69**, 3539-3553. https://doi.org/10.1007/s00484-025-03041-z

[4] Thornton, P.K., van de Steeg, J., Notenbaert, A. and Herrero, M. (2009) The Impacts of Climate Change on Livestock and Livestock Systems in Developing Countries: A Review of What We Know and What We Need to Know. *Agricultural Systems*, **101**, 113-127. https://doi.org/10.1016/j.agsy.2009.05.002

[5] van Wijk, M.T., Rufino, M.C., Enahoro, D., Parsons, D., Silvestri, S., Valdivia, R.O.,

et al. (2014) Farm Household Models to Analyse Food Security in a Changing Climate: A Review. *Global Food Security*, **3**, 77-84. https://doi.org/10.1016/j.gfs.2014.05.001

[6] Wang, H. (2024) γ Distribution for Equilibrium Analysis of Discrete Stochastic Logistic Population Models. arXiv: 2411.10167.

[7] Batardière, B., Chiquet, J., Gindraud, F. and Mariadassou, M. (2025) Zero-Inflation in the Multivariate Poisson Lognormal Family. *Statistics and Computing*, **35**, Article No. 196. https://doi.org/10.1007/s11222-025-10729-0

[8] Limpert, E., Stahel, W.A. and Abbt, M. (2001) Log-Normal Distributions across the Sciences: Keys and Clues. *BioScience*, **51**, 341-352.

[9] Timpson, A., Gillis, R.E., Manning, K. and Thomas, M.G. (2018) Modelling Caprine Age-at-Death Profiles Using the Gamma Distribution. *Journal of Archaeological Science*, **99**, 19-26. https://doi.org/10.1016/j.jas.2018.08.015

[10] Sartore, L., Wei, Y., Abayomi, E., Riggins, S., Corral, G., Bejleri, V., *et al*. (2020) Modeling Swine Population Dynamics at a Finer Temporal Resolution. *Applied Stochastic Models in Business and Industry*, **36**, 1060-1079. https://doi.org/10.1002/asmb.2597

[11] Arlot, S., Marmi, S. and Papini, D. (2019) Coupling the Yoccoz-Birkeland Population Model with Price Dynamics: Chaotic Livestock Commodities Market Cycles. *Nonlinearity*, **32**, 2564-2592. https://doi.org/10.1088/1361-6544/ab0eb7

[12] Hamnett, P.W., Saltré, F., Page, B., Tarran, M., Korcz, M., Fielder, K., *et al*. (2024) Stochastic Population Models to Identify Optimal and Cost-Effective Harvest Strategies for Feral Pig Eradication. *Ecosphere*, **15**, e70082. https://doi.org/10.1002/ecs2.70082

[13] Assogba, G.G.C., Berre, D., Adam, M., Delay, E., Speelman, E. and Descheemaeker, K. (2026) Bridging Gaps in Agro-Ecosystem Integration: A Multi-Level Modelling Study in Semi-Arid Burkina Faso. *Ecological Modelling*, **514**, Article ID: 111478. https://doi.org/10.1016/j.ecolmodel.2026.111478

[14] Cosme, M., Koné, A., Pommereau, F. and Gaucherel, C. (2024) Improving Livelihood through Crop-Livestock Integration: Insights from a Farm Trajectory Model. *Agricultural Systems*, **219**, Article ID: 103949. https://doi.org/10.1016/j.agsy.2024.103949

[15] Dressler, G., Brinkmann, K., Linstädter, A., Menestrey Schwieger, D., Moyo, S.N., Mustelin, K., Rauchecker, M. and Müller, B. (2025) Exploring Livelihood Security and Looming Desertification in Namibia's Communal Rangelands Using an Agent-Based Model. https://www.tropentag.de/2025/abstracts/links/Dressler_EPcW68k2.php

[16] Seo, S.N. and Mendelsohn, R. (2008) Measuring Impacts and Adaptations to Climate Change: A Structural Ricardian Model of African Livestock Management. *Agricultural Economics*, **38**, 151-165. https://doi.org/10.1111/j.1574-0862.2007.00289.x

[17] Burgman, M. (2005) Risks and Decisions for Conservation and Environmental Management. Cambridge University Press https://doi.org/10.1017/cbo9780511614279

[18] Puech, T. (2024) Viability Algorithm to Assess the Robustness and Adaptability of Mixed Herds. https://hal.inrae.fr/hal-04731209

[19] Springbett, A.J., MacKenzie, K., Woolliams, J.A. and Bishop, S.C. (2003) The Contribution of Genetic Diversity to the Spread of Infectious Diseases in Livestock Populations. *Genetics*, **165**, 1465-1474. https://doi.org/10.1093/genetics/165.3.1465

[20] Srivastava, A.K., Rahimi, J., Alsafadi, K., Vianna, M., Enders, A., Zheng, W., *et al*. (2025) Modelling Mixed Crop-Livestock Systems and Climate Impact Assessment in Sub-Saharan Africa. *Scientific Reports*, **15**, Article No. 1399.

https://doi.org/10.1038/s41598-024-81986-8

[21] Moon, G.A. (2003) Intrinsic Priors for Testing Two Lognormal Populations with the Fractional Bayes Factor. *Journal of the Korean Data & Information Science Society*, **14**, 661-671.

[22] Rao, K.A. and D'Cunha, J.G. (2016) Bayesian Inference for Median of the Lognormal Distribution. *Journal of Modern Applied Statistical Methods*, **15**, 526-535. https://doi.org/10.22237/jmasm/1478003400

[23] Dabiré, B.H., Magnini, S. and Sanou, B.W. (2011) Le nouveau régime foncier rural du Burkina Faso à l'épreuve de stratégies locales d'anticipation: cas des villages de Koho, Koumbia et de Yéguéresso. Rapport définitif, 36 p.

[24] Johnson, N.L., Kotz, S. and Balakrishnan, N. (1994) Continuous Univariate Distributions. 2nd Edition, Wiley.

[25] McCullagh, P. and Nelder, J.A. (1989) Generalized Linear Models. 2nd Edition, Chapman & Hall. https://doi.org/10.1201/9780203753736

[26] Lilliefors, H.W. (1967) On the Kolmogorov-Smirnov Test for Normality with Mean and Variance Unknown. *Journal of the American Statistical Association*, **62**, 399-402. https://doi.org/10.1080/01621459.1967.10482916

[27] Stute, W., Manteiga, W.G. and Quindimil, M.P. (1993) Bootstrap Based Goodness-of-Fit-Tests. *Metrika*, **40**, 243-256. https://doi.org/10.1007/bf02613687

[28] Cameron, A.C. and Trivedi, P.K. (2013) Regression Analysis of Count Data. 2nd Edition, Cambridge University Press. https://doi.org/10.1017/cbo9781139013567

[29] Rubinstein, R.Y. and Kroese, D.P. (2016) Simulation and the Monte Carlo Method. Wiley. https://doi.org/10.1002/9781118631980

[30] Efron, B. and Tibshirani, R.J. (1994) An Introduction to the Bootstrap. Chapman & Hall/CRC. https://doi.org/10.1201/9780429246593

[31] Saltelli, A., Ratto, M., Andres, T., Campolongo, F., Cariboni, J., Gatelli, D., *et al*. (2007) Global Sensitivity Analysis. the Primer. Wiley. https://doi.org/10.1002/9780470725184

[32] Ki, J.A. and Traore, D. (2025) Explanatory Factors of Cotton Production in Solenzo of Burkina Faso. Zenodo.